The influence of climate change on Arctic atmospheric rivers and the impacts on sea ice

Rudradutt Thaker

A Thesis submitted in partial fulfillment of

the requirements for the degree of

Master of Science

(Atmospheric and Oceanic Sciences)

at the

University of Wisconsin-Madison

Thesis Declaration and Approval

I, Rudradutt Thaker, declare that this Thesis titled 'The influence of climate change on Arctic atmospheric rivers and the impacts on sea ice' and the work presented in it are my own.

Rudradutt Thaker		
Author	Signature	Date

I hereby approve and recommend for acceptance this work in partial fulfillment of the requirements for the degree of Master of Science:

Stephen Vavrus		
Committee Chair	Signature	Date

Tristan L'Ecuyer		
Faculty Member	Signature	Date

Elizabeth Maroon		
Faculty Member	Signature	Date

Abstract

The influence of climate change on Arctic atmospheric rivers and the impacts on sea ice

by Rudradutt Thaker

Atmospheric rivers (ARs) transport heat and moisture from lower latitudes to the Arctic contributing to Arctic sea ice loss. With ongoing climate warming and declining sea ice, it becomes essential to comprehend the changing dynamics of Arctic ARs. Despite studies indicating increased storms and ARs in recent years, a comprehensive understanding of their changing behavior in a warming climate, seasonal patterns, and impact on sea ice remains incomplete.

Addressing these knowledge gaps, this study investigates the changing dynamics of Arctic ARs in response to a warming climate, delving into the drivers behind these changes and their consequent impacts on sea ice. Utilizing the Community Earth System Model, Version 2 (CESM2), it is found that CESM2 adeptly simulates Arctic ARs when compared to ERA5. In examining the ARs under changing climate conditions, three methods are employed, each modifying the minimum threshold criteria of the detection algorithm. These methods include defining ARs based on present climate thresholds, scaling thresholds with projected moisture changes for the future, and calculating unique thresholds for each decade. The results show that Arctic ARs exhibit heightened frequency and intensity in the future climate, with this increase significantly influenced by the chosen AR definition. Thermodynamics emerge as the primary driver of these changes, although

dynamics also contribute to regional variations. Lastly, the study explores future AR-induced sea-ice changes, revealing a consistent net loss, most pronounced in winter and spring. Notably, these sea-ice impacts are sensitive to the chosen AR definition in a warmer climate.

This research contributes essential knowledge to the evolving relationship between Arctic ARs and sea ice, emphasizing the critical role of sensitivity to results based on AR definition. As the Arctic landscape transforms, understanding these interactions becomes vital for navigating the complex dynamics of climate change.

Dedicated to my parents, Tejal Thaker and Gurudatt Thaker, and my great-grandmother, Vasantben Bhatt.

Acknowledgements

I express my deepest gratitude to my advisor, Steve Vavrus, for introducing me to the fascinating world of science, serving as a mentor, and molding me into a better individual and scientist. I appreciate your guidance in exploring diverse scientific questions while keeping me on track. Your mentorship has been invaluable, and I look forward to continuing to learn from you.

Heartfelt thanks to my collaborators and co-advisors at NCAR, including Christine Shields, Dr. Alice DuVivier, Dr. Marika Holland, and Dr. Laura Landrum. I feel fortunate to have had your guidance at every step, providing knowledge and opportunities to showcase my research. Your feedback and suggestions have played a crucial role in shaping this project.

I extend my appreciation to the members of my committee, Dr. Elizabeth Maroon and Dr. Tristan L'Ecuyer, for their valuable insights and guidance that enhanced this thesis. A special acknowledgment to Dr. Maroon for her project assistance and insights.

My parents have consistently motivated me to pursue my passion, trusting me with my decisions, and I am grateful for their unwavering support. Aayushi, thank you for your constant support and love throughout this graduate school journey and bearing me. It wouldn't have been possible without you all.

Within AOS, I want to thank Evan, Hamish, Natasha, Dan, Yingshun, Marissa, Steph, Clark, Nicolas, Poush, and Connor for all the fun and science conversations, their insights and comments on the thesis, and motivating me to engage in qualitative science. Dr. Hannah Zanowski and Cameron Bertossa, thank you for introducing me to Python and teaching me coding basics. The Oceanographer's group, including Dr. Feng He and Dr. Till Wagner, has been a source of enjoyable scientific conversations. Dr. Kyle Mattingly, your guidance on polar atmospheric rivers has been invaluable. The intriguing questions

from Dr. Ángel Adames-Corralizza, Dr. Daniel Vimont, and Dr. Jon Martin got me thinking from different perspectives and stepped up the quality of this work. Special thanks to Pete, Christi, Scott, Dee, Carolyn, and Kaitlyn for all their assistance.

I want to express my gratitude to friends outside the department, including Dhyey, Sagar, Drashti, Janessa, Michelle, and Becca, for being great friends. Michelle and Becca, thank you for your help with understanding polar atmospheric rivers.

A heartfelt thanks to everyone in my life who has helped me in some way or the other, provided constructive criticism, and contributed to my personal and professional growth.

Thank you Chai for keeping me awake while working on this.

This research was supported by award OPP-2043727 from the National Science Foundation and the high-performance computing support from Casper provided by NCAR's Computational and Information Systems Laboratory, sponsored by the National Science Foundation.

Hum maut ko sapnaa bataakar uth khade honge yahin
Aur honi ko thengaa dikhaakar khilkhilaate jaayenge...

- Piyush Mishra

Contents

List of Figures

List of Tables

Chapter 1

Introduction

1.1 Global Atmospheric Rivers

Atmospheric Rivers (ARs) are narrow, elongated bands of moisture transport that are synoptic in scale and transient in nature. They function as significant water and energy transport conduits and often accompany extratropical cyclones (Ralph et al., 2018, Zhu and Newell, 1998). ARs are often associated with increased cloudiness, carrying substantial heat and moisture. These events account for 90% of total poleward moisture transport (Zhu and Newell, 1998). Globally, ARs play a substantial role in regional hydrology through precipitation (Guan and Waliser, 2015, Paltan et al., 2017, Pan and Lu, 2020, Sousa et al., 2018, Viale et al., 2018). Estimates suggest that ARs contribute substantial precipitation in subtropical and midlatitude regions, up to 30% in California

and European countries (Guan and Waliser, 2015), approximately 20% in Australia (Reid et al., 2022), and around 70% in New Zealand (Prince et al., 2021).

While ARs can play a positive role in hydrology, their impact can also be detrimental. ARs have been identified as instigators of extreme precipitation and flooding on multiple occasions. The economic consequences of these severe AR events are considerable, with individual events surpassing $3 billion and $2 billion in flood damages in the U.S. and Europe, respectively. Notably, over a 40-year span across the U.S., the impacts of 13 ARs individually exceeded the billion-dollar threshold (Corringham et al., 2019, Waliser and Guan, 2017). Moreover, in the Southern Hemisphere, ARs are acknowledged as pivotal contributors to floods in regions such as Australia and New Zealand (Prince et al., 2021, Reid et al., 2021). Hence, ARs contribute both favorably (precipitation in drought prone areas) and unfavorably (floods and extreme rainfall) on a global scale and are extensively studied due to their significant worldwide socio-economic impacts.

What remains understudied, however, are Polar ARs. Although atmospheric rivers are frequently observed in the mid-latitudes of both hemispheres, they occasionally deviate towards the poles, even reaching the interior regions of polar environments. Given the inherently cold and arid nature of polar regions, the influx of moisture and heat brought by ARs has profound impacts on ice sheets, sea ice, and polar ecosystems. For example, ARs cause spikes in temperature, promoting ice melt over Greenland and Antarctica (Mattingly et al., 2018, 2020, 2023, Wille et al., 2019). ARs also contribute to substantial sea ice loss in summer, as evidenced by Wang et al. (2020), and induce significant sea ice

melt during winter, as shown by Zhang et al. (2023) and Li et al. (2022). Francis et al. (2020) found that ARs cause sea ice melt that results in open water and thin ice in the vicinity of traditionally thicker sea ice, resulting in polynya formation.

Collectively, these studies underscore the impacts of ARs in both midlatitude and polar regions and prompt the question: What are the effects of climate change on atmospheric rivers? The overarching goal of this research is to delve into this question specifically for the Arctic region and to understand how Arctic ARs are evolving under changing climate conditions.

1.2 Climate Change impacts on Arctic Atmospheric Rivers

As the global temperature rises due to anthropogenic warming, moisture in the atmosphere increases due to Clausius-Clapeyron relation (Held and Soden, 2006). The increased moisture intensifies the occurrences, intensity, and impact of ARs. Studies show that globally, AR frequency and intensity increase under greenhouse forcing (Allan et al., 2014, Espinoza et al., 2018, O'Brien et al., 2022, Zhang et al., 2021), largely driven by thermodynamic changes. The polar regions also experience similar increases in ARs with changing climate (Kolbe et al., 2023, Ma et al., 2021, Zhang et al., 2023). However, the impacts of circulation changes on ARs pose some complexities. As the westerly jets shift as a response to climate change, a poleward shift of ARs is found over the North Atlantic (Gao et al., 2016). At the same, a small but robust reduction in moisture transport

and an equatorward shift of ARs due to wind changes are found over the North Pacific (for example, Gao et al. (2015), Payne and Magnusdottir (2015), Shields and Kiehl (2016)). Moreover, reduced baroclinic instability, a consequence of polar amplification, makes conditions less favorable for extratropical storms and atmospheric rivers. Hence, as the climate warms, determining the future behavior of ARs becomes challenging.

The need to study atmospheric rivers in the Arctic in a changing climate is underscored by the swift transformations in the region's climate. The recent and substantial reduction in Arctic sea ice (Serreze and Barry, 2011, Stroeve et al., 2008, Walsh et al., 2017) carries profound implications, exerting a pivotal influence on both the global climate system (Francis et al., 2017) and local ecosystems (Woelders et al., 2018). This decline is closely linked to the increasing global air temperatures driven by the surge in greenhouse gas emissions. The resulting decrease in Arctic sea ice, coupled with heightened concentrations of greenhouse gases, manifest in increased frequencies and intensities of extreme events, including cyclones (Rinke et al., 2017), heatwaves (Graham et al., 2017a), moisture intrusion events (Papritz et al., 2022), and ARs in the Arctic (Ma et al., 2021). These changes in extreme phenomena also contribute significantly to amplified sea ice loss (for example, Aue and Rinke (2023), Simmonds and Rudeva (2012), Valkonen et al. (2021), Woelders et al. (2018)), augmented precipitation, and heightened risks of flooding (Bachand and Walsh, 2022), thereby yielding substantial repercussions for ecosystems. While extensive research has delved into Arctic cyclones, heatwaves, and their consequences (for example, Aue and Rinke (2023), Graham et al. (2017b), Papritz et al. (2022), Rinke et al.

(2017), Valkonen et al. (2021)), the examination of Arctic ARs remains relatively nascent in scientific inquiry.

While several studies have specifically investigated Arctic AR changes, such as those conducted by Ma et al. (2021), Zhang et al. (2023), and Kolbe et al. (2023), they also serve as catalysts for additional research inquiries. Zhang et al. (2023) highlighted a substantial uptick in Arctic AR frequency from 1980-2020 using reanalysis and climate models, prompting subsequent investigation into their future trajectories. Ma et al. (2021) initially tackled this question by utilizing Polar Amplification Model Intercomparison Project (PAMIP) model runs, revealing that sea ice loss influences Arctic ARs by inducing poleward shifts in the Pacific sector and a concomitant equatorward shift in the Atlantic sector. Kolbe et al. (2023) employed EC-Earth2.3 large ensembles to scrutinize Arctic AR dynamics across present and future climates, revealing that AR changes are predominantly governed by thermodynamic shifts in a warming scenario.

Previous studies, such as Ma et al. (2021), conducted targeted model experiments by imposing present-day and future sea ice concentrations from CMIP5 models into PAMIP models to investigate the impact of sea ice on Arctic ARs. Additionally, Kolbe et al. (2023) prescribed a global mean surface temperature increase of 2°C and 3°C for specific time periods to investigate the changes in ARs in a warming climate. These distinct approaches prompts a pertinent question regarding the response of ARs and their impacts under transient climate changes driven by continuous CO2 forcing.

Moreover, while existing research has examined Arctic AR changes during winter (Ma et al., 2021, Zhang et al., 2023) and annually (Kolbe et al., 2023), a discernable gap remains in comprehensively elucidating the seasonal variations of Arctic ARs. This gap is noteworthy considering the evolving seasonality in the Arctic due to climate change and the potential sensitivity of AR thermodynamic and dynamic variations to these seasonal shifts. Therefore, additional investigation is needed into seasonal variations of Arctic ARs using a coupled climate model in future simulations.

1.3 Arctic AR Impacts

Arctic atmospheric rivers are frequently implicated in the adverse effects of global warming, including the melting of Greenland ice sheets (Mattingly et al., 2018, 2020, 2023), sea ice loss (Gimeno et al., 2015, Li et al., 2022, Wang et al., 2020, Zhang et al., 2023), and occurrences of extreme precipitation and flooding (Nash et al., 2018). The unique topography and pronounced land boundaries of Greenland provide ideal conditions for ARs to undergo orographic lift during landfall, instigating substantial alterations to the surface mass balance (SMB) through precipitation and modifications in surface energy balance. For instance, Mattingly et al. (2018) observed that ARs typically yield SMB gains in the GrIS ablation zone during non-summer seasons and in the accumulation zone throughout the year. However, during years of enhanced moisture transport, intense summer SMB losses in the ablation zone outweigh the positive AR contributions to SMB in other regions and seasons.

Additionally, Arctic ARs induce significant changes in sea ice dynamically by impacting sea ice movement and thermodynamically by enhancing downwelling longwave radiation, heat advection, and precipitation (Li et al., 2022). These processes amplify the prevailing trend of sea ice loss in the Arctic. Despite sea ice typically growing during boreal winter, winter ARs impede sea ice growth, resulting in a smaller areal sea ice maximum. As observed by Zhang et al. (2023), recurrent ARs during the winter season exert a pronounced melting effect on sea ice, primarily through increased downwelling longwave radiation, hindering seasonal recovery.

The anticipation is that, as the climate warms, considerable sea ice loss occurs, rendering it thinner and more susceptible to extreme weather events like ARs. In the future, the signal of sea ice loss is expected to intensify due to the warm climate and increased extremes, but the impacts of ARs on sea ice are intricately linked to the definition of ARs in a changing climate. The magnitude of this impact is highly contingent upon the chosen definition of atmospheric rivers, whether fixed to historical conditions or adjusted to moister climates in the future (Kolbe et al., 2023) (Section 2.3). Identifying and interpreting these methodological distinctions are crucial for a comprehensive and accurate assessment of the impacts of a changing climate on Arctic ARs and their interactions with sea ice.

1.4 Research Objectives

In this study, we examine the interplay between the evolving climate and Arctic ARs, including their changes in seasonality and impacts on sea ice, to address the following questions :

1. **Model Validation:** How faithfully does a state-of-the-art global climate model represent ARs in the Arctic?

2. **Future Climate Changes:** What are the projected changes in ARs under future climate conditions, particularly in the context of global warming?

3. **Role of moisture in AR changes:** How does the increase in moisture under future climate conditions contribute to the projected changes in Arctic Atmospheric Rivers?

4. **Threshold Sensitivity:** To what extent are the outcomes influenced by the choice of moisture transport thresholds used to define ARs?

5. **AR Impacts on Sea Ice:** What is the sensitivity of sea ice and its variability to the choice of atmospheric river detection tool (ARDT)?

This multifaceted approach is necessary for a comprehensive understanding of the intricate relationship between Arctic ARs and a changing climate, addressing both the model's fidelity and the nuanced impacts associated with varying detection thresholds.

Chapter 2 will describe the data and methods employed in this study to detect ARs, their changing nature, and impacts. Chapter 3 will highlight the findings on model evaluation, shifts in Arctic ARs due to climate change, and their effects on sea ice. Chapter 4 provides a discussion of the results, including caveats. Chapter 5 presents conclusions and future work.

Chapter 2

Data and Methods

2.1 Climate Model Data and Reanalysis Data

The Community Earth System Model Version 2 - Large Ensemble (CESM2/LENS2) (Danabasoglu et al., 2020, Rodgers et al., 2021) is used to investigate the behavior of Arctic ARs in the changing climate. LENS2 consists of 100 ensemble members at a nominal 1-degree spatial resolution, with a historical run (spanning 1850-2014) under Coupled Model Intercomparison Project version 6 (CMIP6) historical forcings and a future run (spanning 2015-2100) under the Shared Socioeconomic Pathway - 370 (SSP370) future radiative forcing scenario. The selection of CESM2/LENS2 is justified by its extensive ensemble size, high spatial resolution, and the precedent set by previous studies using CESM2 for investigating extreme events such as Arctic cyclones (Clancy et al., 2022) and Arctic ARs (Zhang et al., 2023).

To discern ARs in the Arctic, we calculate 6-hourly vertically integrated meridional vapor transport (vIVT) as detailed in Equation 2.1 during the model runs.

$$vIVT = \frac{-1}{g} \int_{1000hPa}^{200hPa} q_p v_p dp \tag{2.1}$$

To disentangle the contributions of thermodynamics and dynamics to changes in ARs in future climates, we incorporate monthly integrated water vapor (IWV) data. To explore the impacts of Arctic ARs on sea ice (Section 3.3), we use daily sea ice concentration (SIC), regridded to standard LENS2 1-degree grid for consistency. The 6-hourly vIVT data is accessible for only 40 ensemble members in LENS2 runs; consequently, these same 40 members are employed for all variables in the present study. Notably, these 40 ensemble members are derived from the modified biomass burning simulations. In these simulations, the initial biomass burning data used in CMIP6 simulations undergoes smoothing via an 11-year running mean. This smoothing process is applied in conjunction with other model corrections, as elucidated in Rodgers et al. (2021), and includes the preservation of additional variables for comprehensive analysis.

To gauge the realism of LENS2 in simulating ARs, we employ the European Centre for Medium-Range Weather Forecasts (ECMWF) Reanalysis v5 (ERA5) dataset (Hersbach et al., 2020). Although the ERA5 dataset spans from 1940 to the present, our study focuses on the data produced by the Atmospheric River Tracking Method Intercomparison Project (ARTMIP) (Shields et al., 2018) covering the period from 1980 to 2014. This

timeframe aligns with the LENS2 historical simulation interval (1980-2014) utilized in our investigation. The ARTMIP dataset encompasses pre-calculated variables, including vertically integrated meridional vapor transport (vIVT), vertically integrated vapor transport (IVT), and vertically integrated water vapor (IWV), specifically tailored for AR detection purposes.

Considering ERA5's finer spatial resolution of 0.25° and a temporal resolution of 1 hour, we regridded the dataset to conform to the standard LENS2 1° grid with a 6-hourly temporal resolution. Refer to Section 3.1 for detailed validation results.

2.2 Atmospheric River Detection Tool (ARDT) in Present Climate (1980-2014)

Global atmospheric rivers are quantitatively defined using various tracking algorithms specifically designed for detecting either global or regional atmospheric rivers. These algorithms, integral to AR studies, apply different thresholds for detection and vary in parameters such as length, orientation, duration, area, and the physical parameter of detection. This variability underscores the high sensitivity of atmospheric river results to the choice of the algorithm employed (Rutz et al., 2019).

In this study, a detection algorithm tailored for polar environments, based on vIVT between latitudes 42.5°N and 85°N is used. ARs are identified using a 98th percentile threshold applied to vIVT at 6-hour intervals, with thresholds recalculated monthly to

accommodate seasonal fluctuations in vapor transport (Wille et al., 2021). Additionally, a minimum meridional length of 20 degrees is imposed for the detection of filaments defined as an AR. This method, characterized by a notably higher threshold, identifies fewer ARs in the Arctic compared to other ARDTs (Rutz et al., 2019, Shields et al., 2018). However, it proves effective in capturing polar ARs as shown by (Maclennan et al., 2022, Wille et al., 2019, 2021).

2.3 Atmospheric River Detection and Tracking Algorithm in Future Climate (2015-2100)

Examining ARs in a changing climate necessitates addressing the subjective definition of extreme events in such a context. This consideration extends beyond ARs to other extremes, including marine heatwaves and cyclones. The central question revolves around whether the definition of extremes in the future climate should be contingent on projected climate change or grounded in the present climate state. For ARs, this differentiation is articulated through the terms 'fixed relative' and 'relative relative' (O'Brien et al., 2022). In the former, the threshold employed for AR detection remains constant over time (specifically calibrated to the present climate), yet has spatial variability (unique threshold for each location). Conversely, in the latter, the threshold changes both temporally and spatially.

The adoption of both definitions, 'fixed relative' and 'relative relative,' allows for a nuanced exploration of the drivers influencing changes in ARs amid a changing climate.

This methodological approach not only adds depth to our understanding of AR dynamics but also sheds light on the interplay between time-dependent and spatially variable thresholds in shaping the evolving nature of ARs under changing climatic conditions.

In this study, for the detection of ARs in the future warming climate under the SSP370 scenario, three distinct methods based on the Wille algorithm (described in Section 2.2) are employed.

1. **Historical Threshold (Hist_Thresh) :** To quantify future changes in ARs based on the current climate (1980-2014), the vIVT thresholds calculated for this period using individual ensemble members are also applied to detect ARs until the end of the century (2100). This method falls under the category of "fixed relative," where the threshold varies relative to location but remains constant over time (O'Brien et al., 2022).

2. **Moisture Scaled (IWV_Scaled) :** To control for the increasing background moisture due to greenhouse warming, historical thresholds (1980-2014 - same as Hist_Thresh method) are scaled with changes in IWV accounting for the background changes in moisture. Ratios of IWV changes are calculated with reference to 1980-2014, for each grid point and month in the future climate scenario using the ensemble average across 40 members. The historical vIVT thresholds are then multiplied by these ratios to scale the detection threshold based on climatological moisture changes. This method falls under "relative relative," where the threshold varies both in time and space (O'Brien et al., 2022).

3. **Decadal Window (Decadal_Win) :** To address the projected changes in vIVT, a running percentile approach to compute thresholds within a 10 year moving window was used initially. However, the computational demands of applying a running percentile to a 6 hourly dataset proved to be challenging. Hence, a moving vIVT threshold is defined for each decade, resulting in a unique threshold for each period (e.g., 2015-2024, 2025-2034, etc.). This method incorporates scaling for both moisture and northward velocity, as vIVT is a function of both specific humidity and meridional wind velocity (Equation 2.1). This method also falls under the "relative relative" category (O'Brien et al., 2022).

Figure 2.1 illustrates the temporal evolution of threshold changes for a randomly selected location, employing different methods described above. Both the Decadal_Win method and IWV_Scaled method exhibit variations over time. In contrast, the Hist_Thresh method maintains a constant threshold throughout the entire time period. The limitations of and insights from each algorithm are discussed in the Results (Section 3.2) and Discussion (Chapter 4) section.

To discern individual ARs in the Arctic and conduct an in-depth analysis of alterations in frequency, duration, intensity, and their impacts on sea ice for each event, the StitchBlob algorithm from TempestExtremes (Ullrich et al., 2021) is utilized. StitchBlob operates as a node-connecting algorithm, facilitating spatial and temporal tracking of identified ARs. This process assigns unique tags and names to categorize them as individual ARs, enabling a detailed examination of each AR event. Moreover, a supplementary filter is

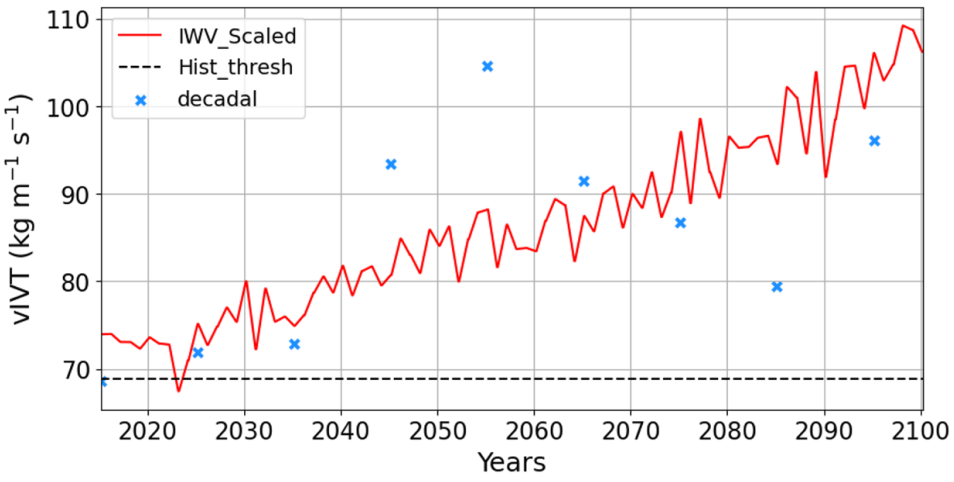

FIGURE 2.1: The vIVT threshold calculated for a random location (85.29°N and 100°E) in the Arctic for the month of March using three methods : red line (IWV_Scaled), black dashed line (Hist_Thresh), and the markers 'x' (Decadal_Win).

applied to isolate ARs with a duration exceeding 12 hours, ensuring a focused investigation into individual AR events.

To examine the seasonality of Arctic ARs and changes in future, the seasons are shifted by a month to group months with similar patterns into each season. The defined seasons include Winter (January, February, March), Spring (April, May, June), Summer (July, August, September), and Fall (October, November, December). For regional analysis, the study categorizes regions into four sectors, as illustrated in Figure 2.2, using the name of each sector to describe the region.

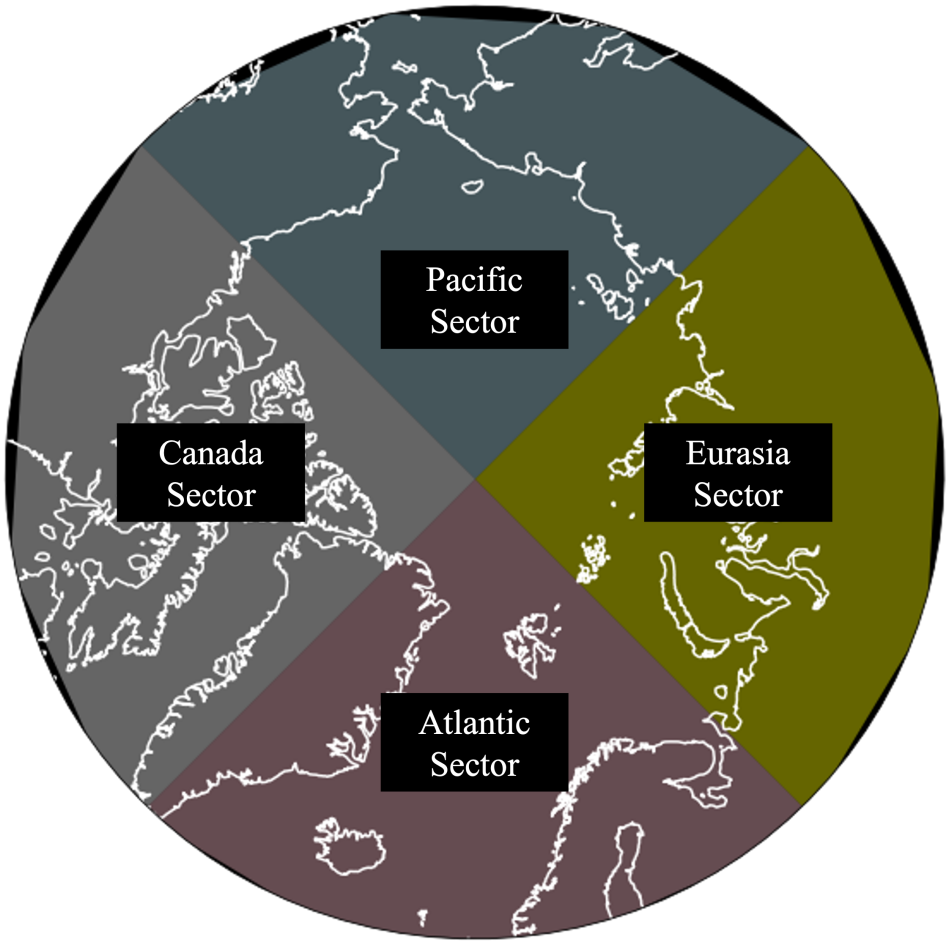

FIGURE 2.2: The Arctic region is divided into four sectors, each spanning from 60°N to 90°N latitude. These sectors are labeled as follows: 1) Atlantic Sector (red : 45°W to 45°E), 2) Eurasia Sector (yellow : 45°E to 135°E), 3) Pacific Sector (blue : 135°E to 135°W), and 4) Canada Sector (white : 135°W to 4°5W).

2.4 Impacts on Sea Ice

To examine the effects of ARs on sea ice, daily sea ice concentration outputs from CESM2 is used. Given the daily nature of the sea ice concentration (SIC) data, only ARs with duration exceeding 12 hours are investigated to ensure a comprehensive representation of sea ice impacts. Subsequently, the area covered by an AR during its occurrence is examined to quantify the sea ice changes associated with AR events. Detailed explanation with an example can be found in Section 3.3.1.

Chapter 3

Results

3.1 Comparing ARs in CESM2 with ERA5:

This section delves into the intricacies of AR frequency and poleward moisture transport (PMT) in the Arctic during the present climate period spanning 1980-2014. The assessment of CESM2 involves contrasting it with ERA5 data, serving as the observational benchmark. To offer a comprehensive overview of AR attributes, both frequency and PMT metrics are considered. The fundamental question guiding this investigation is:

- **Model Validation:** To what extent does this state-of-the-art global climate model faithfully capture the observed characteristics of atmospheric rivers in the Arctic?

3.1.1 AR Frequency

Figure 3.1 provides an overview of the annual frequency of atmospheric rivers (AR) measured in AR-days/year, from ERA5 (Figure 3.1a) and CESM2 ensemble mean (Figure 3.1b). Evaluating CESM2 solely using its ensemble mean is not ideal, as ERA5's AR frequency is influenced by both internal variability and external forcing. To discern model biases apart from internal variability, all 40 ensemble members are individually compared with ERA5. Model bias is identified when the observed AR frequency in ERA5 falls outside the ensemble range in CESM2. The average model bias is then calculated using the ensemble mean and shown as 'Diff' in Figure 3.1 and Figure 3.2. Figure 3.3 and Table 3.1 summarizes the comparison of CESM2 and ERA5.

The Arctic experiences sporadic AR occurrences, registering an average annual frequency of 1.54 AR-days/year according to ERA5, with some regions reaching 3.17 AR-days/year. Seasonal differences, as depicted in Figure 3.2a-d, underscore distinctive patterns with heightened AR occurrences during winter in ERA5 (average frequency of 0.49 AR-days/year in OND) compared to the relatively subdued summer (average frequency of 0.25 AR-days/year in JAS).

Particularly during winter in ERA5, noteworthy AR hotspots emerge in South Greenland and regions proximate to the North Pacific, encompassing the Beaufort, Chukchi, and East Siberian seas (Figure 3.2a, b). This elevated frequency during winter is attributed to intensified baroclinicity and an increased prevalence of storms in the Arctic,

as documented by Valkonen et al. (2021). Conversely, ARs exhibit reduced frequency during the spring and summer (Figure 3.2c, d), likely due to a diminished baroclinic environment.

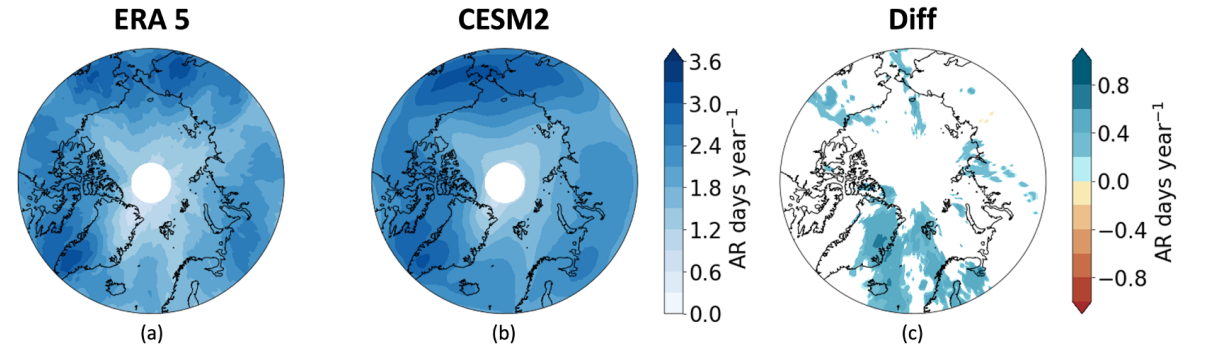

FIGURE 3.1: Annual atmospheric river (AR) frequency shown as AR-days/year from 1980 to 2014 as depicted in (a) ERA5, and (b) the ensemble mean CESM2. (c) illustrates the disparity in AR frequency between CESM2 and ERA5 (CESM2 - ERA5) or 'Diff.' In (c), shades of blue indicate an increased AR frequency in CESM2 vs. ERA5, while shades of brown denote a decreased frequency.

The analysis of annual and seasonal ensemble mean AR frequency for CESM2 (Figure 3.1 and Figure 3.2) provides insights into the model's performance in representing Arctic ARs. Seasonally, CESM2's ensemble mean correctly represents the heightened AR frequency during winter, in contrast to the subdued occurrences observed in summer months. The spatial distribution of ARs is consistently well-captured across all seasons, with distinct hotspots near southern Greenland, the Bering Strait, and the North Atlantic.

Moreover, in comparison to ERA5 (Figure 3.1c), CESM2 performs commendably but shows a higher count of ARs in the Atlantic sector. However, upon closer examination of seasonal variations, CESM2 exhibits more noticeable biases. In fall and winter (Figure 3.2i, Figure 3.2j), CESM2 generally performs well, with scattered biases near the

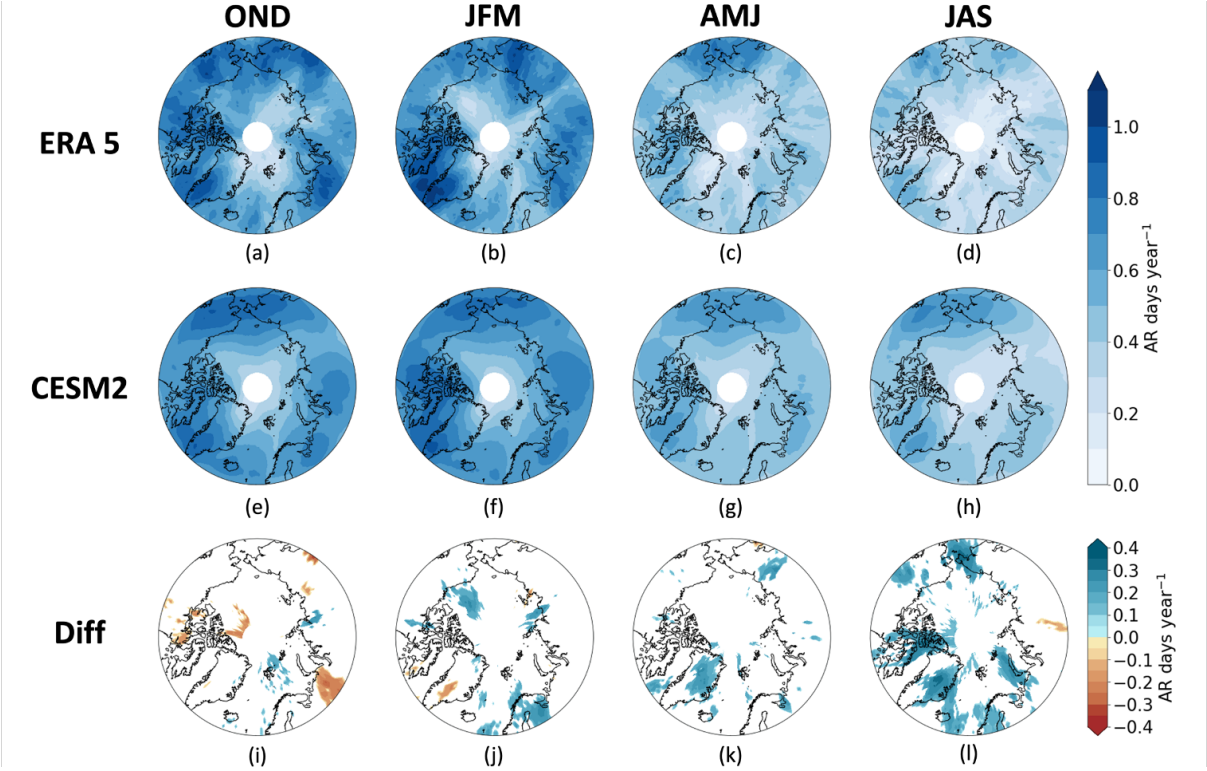

FIGURE 3.2: Seasonal atmospheric river (AR) frequency shown as AR-days/year from 1980 to 2014 is depicted in panels (a-d) for ERA5 and panels (e-h) for the ensemble mean CESM2. Panels (i-l) illustrate the disparity in AR frequency between CESM2 and ERA5 (CESM2 - ERA5) or 'Diff.' In (i-l), shades of blue indicate an increased number of ARs in CESM2 vs. ERA5, while shades of brown denote a decreased number. Each column represents seasonal variations.

Beaufort and Barents Seas in winter. In spring, CESM2 displays a positive bias (more ARs than ERA5) over Greenland. In contrast to other seasons, the most substantial biases emerge in summer (Figure 3.2l), when CESM2 tends to generate more ARs over the North Atlantic, East Greenland, Canadian Archipelagos, and North Pacific.

Figure 3.3 and Table 3.1 demonstrate that, on the whole, CESM2 accurately reproduces the averaged AR frequency across the Arctic, with notable consistency in fall. Winter and spring seasons exhibit a slight positive bias compared to ERA5. The ensemble range

successfully captures ERA5 values for spring, while in winter, although very close, the ensemble range falls slightly short of capturing ERA5 values. The most prominent and distinct model bias is evident during the summer season, with both the ensemble mean and range higher than ERA5.

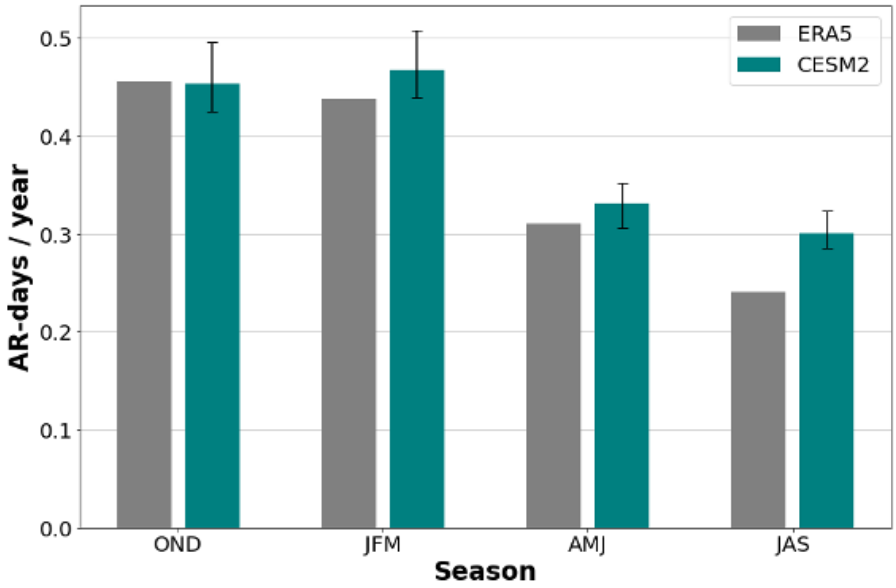

FIGURE 3.3: Spatially averaged Arctic AR frequency for all seasons in ERA5 and CESM2 for the period 1980-2015. The error bars represent the ensemble range of CESM2 using 40 ensemble members.

Considering studies by Zhang et al. (2023), emphasizing the crucial role of ARs in driving sea-ice melt in the Atlantic and influencing the surface mass balance (SMB) of the Greenland ice sheet (Mattingly et al., 2018, 2020, 2023), acknowledging these biases becomes imperative.

These biases can be linked to the warm bias in CESM2 (Chapter 4), leading to excessive moisture, warmth, and potentially more ARs in all seasons. This specific bias is most prominent in summer, aligning with CESM2's greatest positive bias of ARs during this

	OND	JFM	AMJ	JAS
ERA5	0.489	0.438	0.310	0.240
CESM2 Mean	0.453	0.468	0.332	0.301
CESM2 Ensemble Spread	0.425 - 0.496	0.439 - 0.508	0.306 - 0.352	0.285 - 0.324
Diff (%) Mean	-0.52	6.60	6.51	22.38
Diff (%) Ensemble Spread	(-6.97) - 8.55	0.23 - 14.78	(-1.4) - 12.39	17.08 - 29.59

TABLE 3.1: Average Arctic Atmospheric River (AR) frequency expressed in AR-days/year across different seasons in ERA5 and CESM2 from 1980 to 2015. The provided percentage illustrates the difference between CESM2 and ERA5 (CESM2 - ERA5). The ensemble range indicates the minimum and maximum values observed across the ensemble members.

season. Furthermore, the heightened frequency of ARs over Greenland, as captured by CESM2, introduces a bias that may impact the interpretation of ARs' role in summer precipitation and changes in net surface mass balance over Greenland. Notably, this bias has implications for the onset of sea-ice melt due to ARs and the examination of sea-ice changes during summer months.

3.1.2 Evaluating Poleward Moisture Transport (PMT) Intensity in ARs

Beyond frequency, an integral aspect for consideration in atmospheric rivers analysis is the volume of moisture transported during these events. This metric plays a pivotal role

in influencing precipitation characteristics, sea ice changes, and ice sheets. Figure 3.4 presents the annual average poleward moisture transport (PMT) during ARs, comparing ERA5 (Figure 3.4a) and CESM2 (Figure 3.4b) across the Arctic. A detailed breakdown by season is presented in Figure 3.5, and a summary of ERA5 and CESM2 comparisons across all seasons for PMT in ARs is presented in Figure 3.6 Table 3.2. The model biases are calculated the same way as calculated for AR frequency in the Section 3.1.1 and are shown as 'Diff' in Figure 3.4 and Figure 3.5.

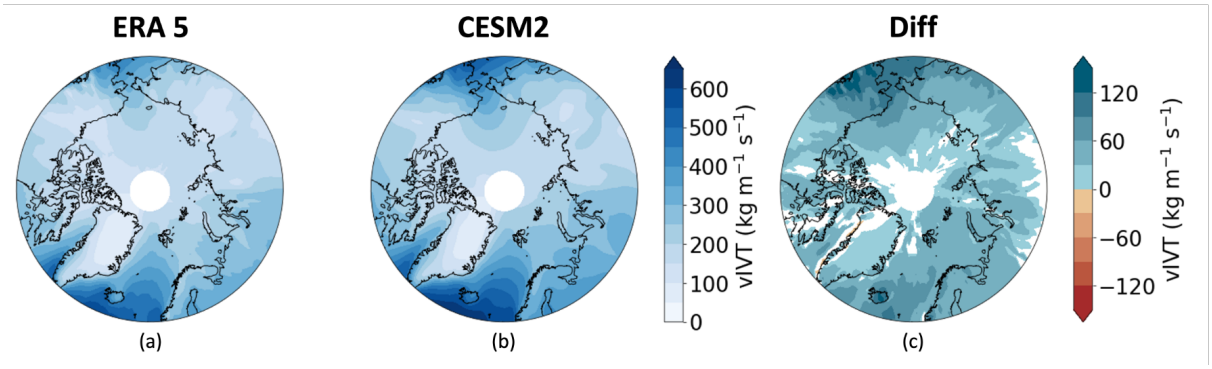

FIGURE 3.4: Average poleward moisture transport (PMT) (kg m-1s-1) in atmospheric rivers from 1980 to 2014 depicted in (a) ERA5, and (b) ensemble mean CESM2. Panel (c) illustrates the disparity in AR-associated PMT between CESM2 and ERA5 (CESM2 - ERA5) or 'Diff.' In (c), shades of blue indicate more PMT in ARs.

The regions characterized by higher AR frequency, such as South-West Greenland and nearby regions, exhibit a correspondingly larger PMT (Figure 3.3a, b), underscoring the pivotal role of these locations in moisture transport dynamics. In contrast, the Atlantic sector, while not experiencing the highest frequency of ARs, does have the most substantial PMT, emphasizing the unique dynamics at play in this region.

On an annual basis CESM2 consistently exhibits higher PMT across the Arctic with the

Pacific sector showing the largest biases when compared to ERA5 (Figure 3.4c). This correspondence is notable, as the Pacific sector does not show large biases in AR frequency (Figure 3.1c).

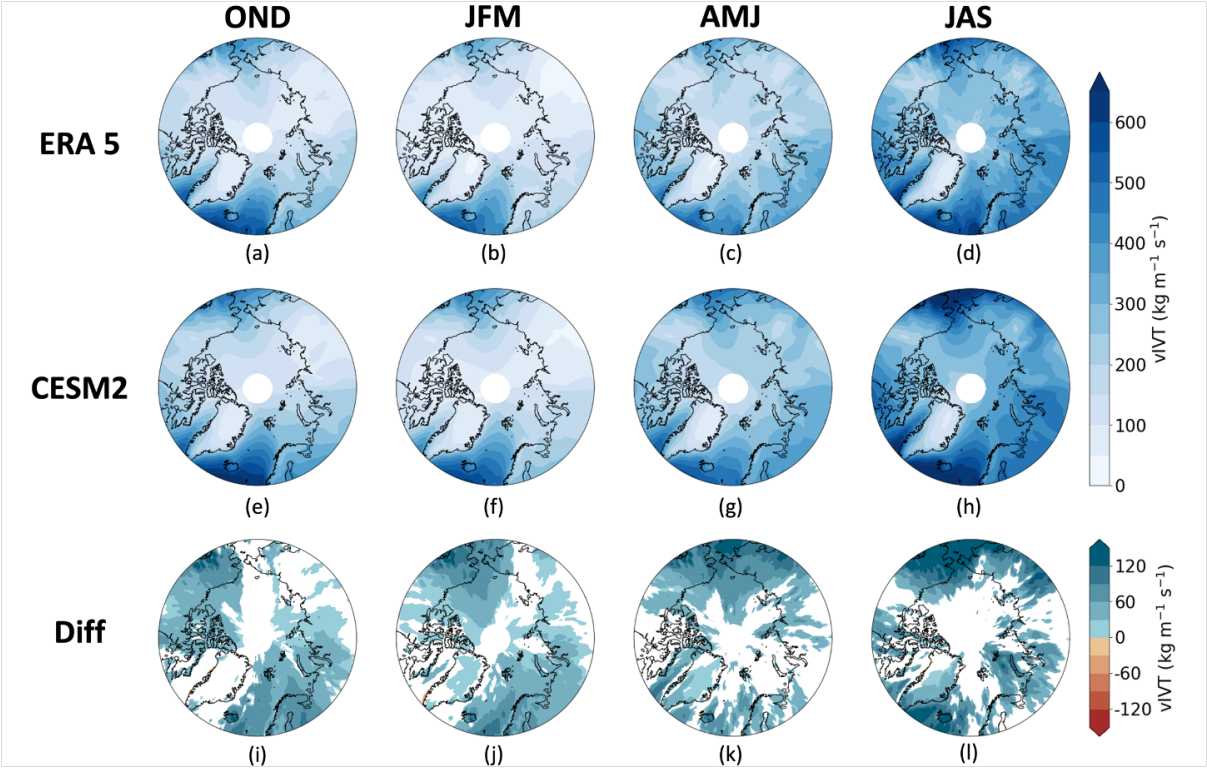

FIGURE 3.5: Poleward moisture transport (PMT) (kg m-1s-1) in atmospheric rivers from 1980 to 2014 is depicted in panels (a-d) for ERA5 and panels (e-h) for the ensemble mean CESM2. Panels (i-l) illustrate the disparity in AR-associated PMT between CESM2 and ERA5 (CESM2 - ERA5) or 'Diff.' In (i-l), shades of blue indicate more PMT in ARs in CESM2.

Across all the seasons, the biases observed in PMT (Figure 3.5i-l) show a consistent overestimation by CESM2 in the Arctic. Similar to the AR frequency, the biases identified in summer are larger than any other season (Figure 3.5l). Figure 3.6 and Table 3.2 summarizes the comparison of CESM2 and ERA5, showing an elevated AR-associated PMT surpassing ERA5 values in all seasons. This notable excess in simulated PMT shows

potential model biases in CESM2, which largely exist due to an overly warm and moist Arctic depicted by CESM2 (Chapter 4).

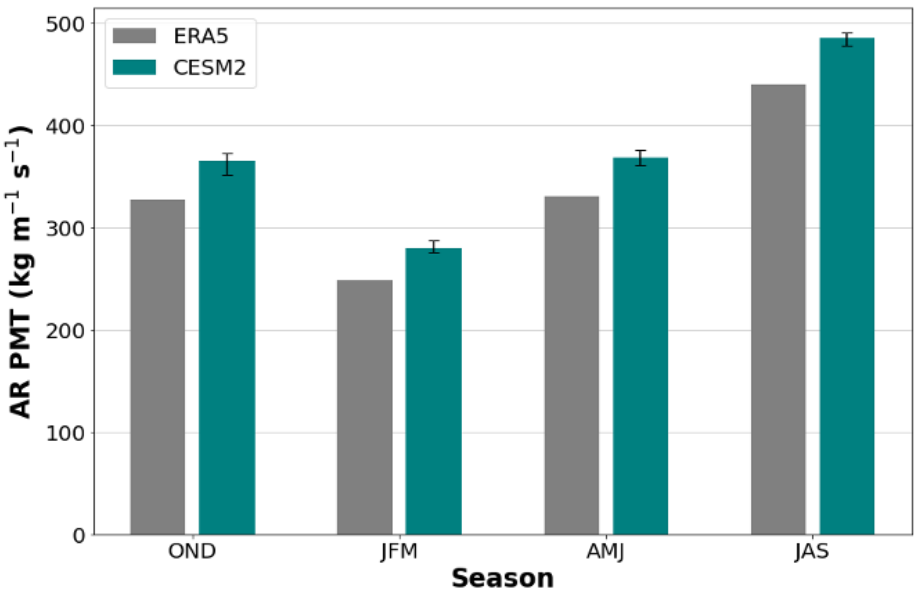

FIGURE 3.6: Spatially averaged Arctic AR-related poleward moisture transport (PMT) for all seasons in ERA5 and CESM2 for the period 1980-2015. The error bars represent the ensemble range of CESM2 using 40 ensemble members.

	OND	**JFM**	**AMJ**	**JAS**
ERA5	269.089	202.799	283.443	388.930
CESM2 Mean	303.411	233.630	320.670	433.282
CESM2 Ensemble Spread	292.339 - 308.668	229.542 - 239.878	314.933 - 327.758	425.831 - 439.192
Diff (%) Mean	11.99	14.13	12.32	10.79
Diff (%) Ensemble Spread	8.23 - 13.70	12.37 - 16.75	10.52 - 14.50	9.06 - 10.79

TABLE 3.2: Similar to table 1 but for spatially averaged Arctic AR related poleward moisture transport (PMT) expressed in $kgm^{-1}s^{-1}/year$.

3.1.3 Summary

The findings presented in this section demonstrate that CESM2 adequately reproduces the characteristics of Arctic atmospheric rivers when contrasted with the ERA5 reanalysis dataset. Overall, CESM2 exhibits a proficient representation of both the frequency of ARs and the associated PMT. While the annual discrepancies are relatively modest, notable seasonal biases are observed. CESM2 performs well in simulating Arctic ARs compared to ERA5 in fall and with small positive biases in winter and spring seasons. However, CESM2 tends to overestimate AR-associated Poleward Moisture Transport (PMT) across all seasons and throughout the Arctic. The most notable disparity in AR frequency and associated PMT is observed in summer.

3.2 Future Climate and ARs

This section provides an overview of the observed alterations in ARs between the future and present climate periods in CESM2. The examination specifically targets variations in AR frequency, duration, and intensity across different seasons, to illustrate seasonal nuances. The comparative analysis aims to identify the underlying factors steering these changes and understand the role of moisture variations in influencing Arctic ARs in future climate. Additionally, the section highlights the sensitivity of future AR changes to the definition of ARs (Section 2.3). The primary questions addressed in this section include:

- **Future Climate Changes:** What are the projected changes in ARs under future climate conditions, particularly in the context of global warming?

- **Role of moisture in AR changes:** How does the increase in moisture under future climate conditions contribute to the projected changes in Arctic Atmospheric Rivers?

- **Threshold Sensitivity:** To what extent are the outcomes influenced by the choice of moisture transport thresholds used to define ARs?

3.2.1 Changes in Arctic AR Frequency and Duration

As the climate undergoes warming, an anticipated rise in Arctic AR frequency in CESM2 aligns with previous studies (Allan et al., 2014, Espinoza et al., 2018, Kolbe et al., 2023, O'Brien et al., 2022, Zhang et al., 2021). However, the extent of this increase in future ARs hinges on their definition in a changing climate. Figure 3.7 and Figure 3.8 present the changes in AR counts per year and the average AR duration, respectively, across the Arctic, employing three distinct methods outlined in Section 2.3. Trends are determined through linear least-squares regression, and their statistical significance is assessed using a Wald's test with a significance threshold ($p - value < 0.01$).

Hist_Thresh emerges with the highest number of ARs in the future across all seasons, primarily because its definition remains rooted in the present climate period (1980-2014). Notably, by the end of the century, this method captures more ARs during summer ($\approx$ 120 ARs) with an increasing trend of approximately 1 AR/year. In contrast, the winter season has around 100 ARs with a trend of 0.613 ARs/year. This contrasts with the present climate, when AR frequency is higher in autumn and winter (Figure 3.2,

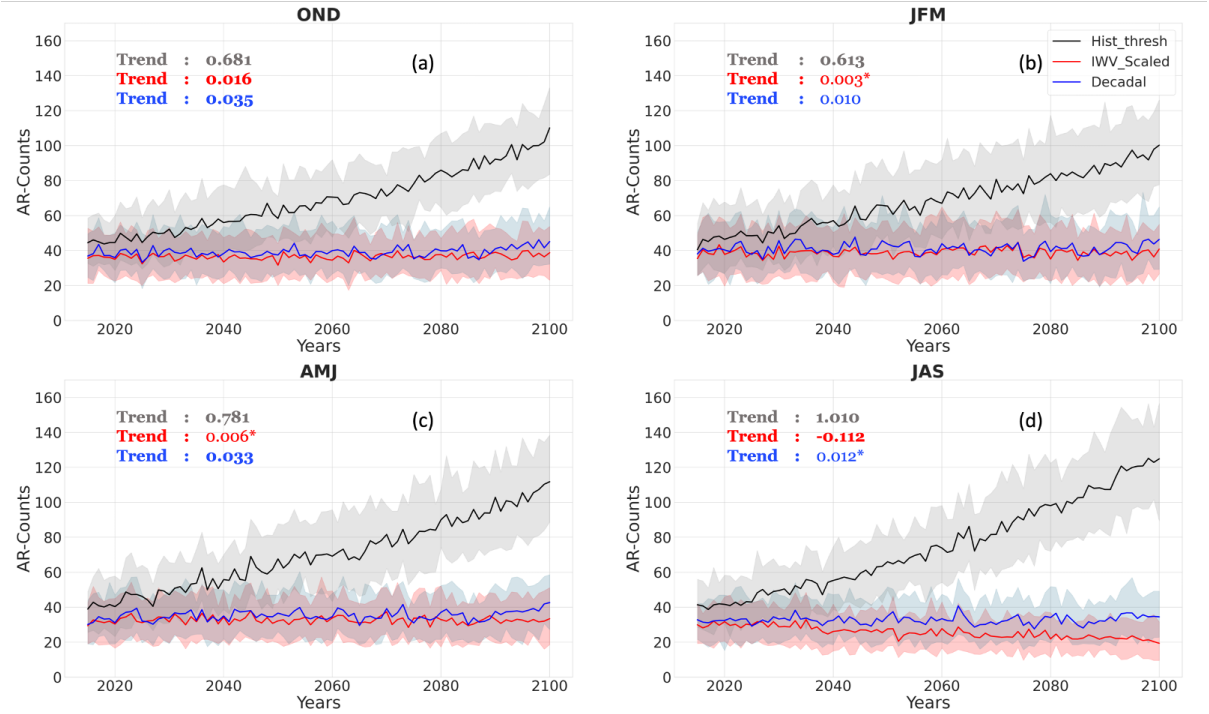

FIGURE 3.7: Arctic atmospheric river occurrences per year from 2015-2100 across seasons during (a) October-November-December (OND), (b) January-February-March (JFM), (c) April-May-June (AMJ), (d) July-August-September (JAS). Solid lines depict the ensemble mean for Hist_Thresh (black), IWV_Scaled (red), and Decadal_Win (blue), while shaded regions in corresponding colors represent the ensemble spread (lower bound : 10th percentile, upper bound : 90th percentile). The trends for each method are shown as AR-counts/year, with colors corresponding to their respective methods. Statistically non-significant trends are denoted with an asterisk.

Table 3.1). Although Hist_Thresh captures ARs associated with anomalous poleward moisture transport, it predominantly reflects an increase in local moisture content, resulting in a higher number of ARs in the Arctic. Concurrently, as AR counts increase, the average duration of ARs also lengthen (Figure 3.8, similar trend in all seasons), indicating a future trend of heightened frequency and longer duration in ARs in the Arctic.

Contrarily, when the inherent increase in moisture is accounted for, mitigating the dominating effect of moisture enhancement, the subsequent surge in AR frequency becomes

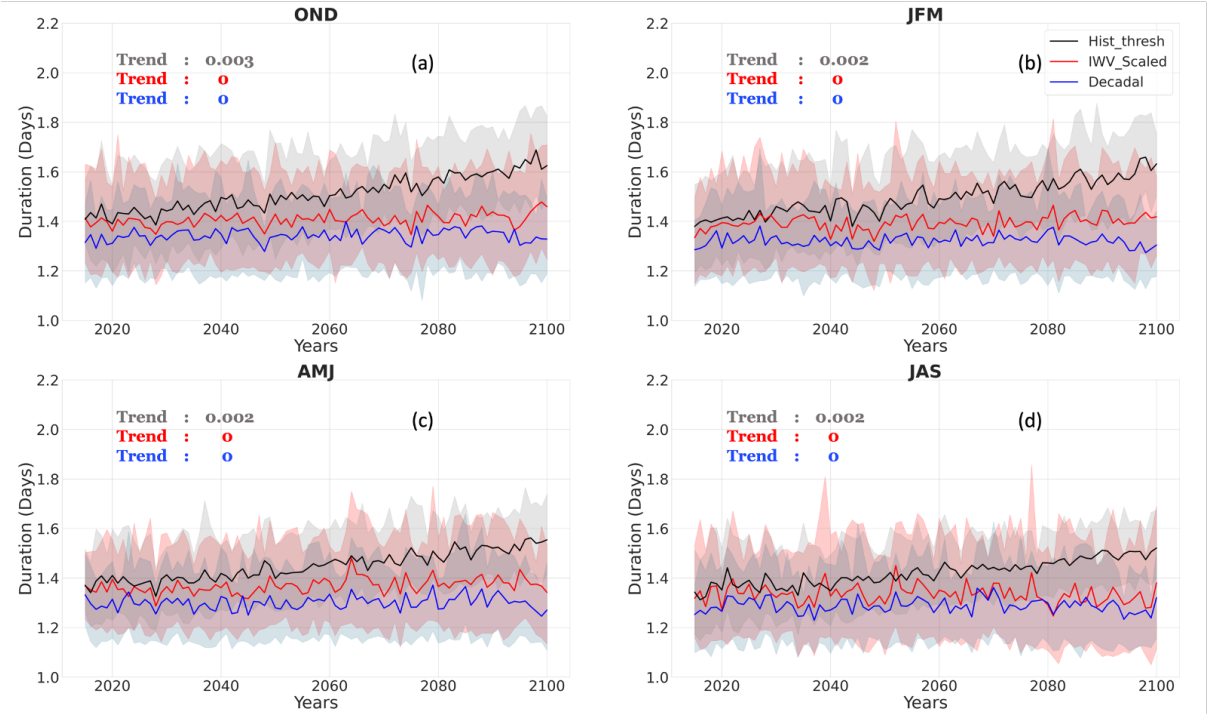

FIGURE 3.8: Same as Figure 3.5 but for average Arctic atmospheric river duration. The trends for each method are shown as days/year, with colors corresponding to their respective methods. Statistically non-significant trends are denoted with an asterisk.

less prominent. Methods IWV_Scaled (red) and Decadal_Win (blue) effectively account for the background moisture, revealing minimal or no discernible trends in the number of AR events or their durations across individual seasons (Figure 3.7 and Figure 3.8). The Decadal_Win method captures a comparable or slightly higher number of ARs than IWV_Scaled (Figure 3.7). Notably, the seasonal patterns by the end of the century, contradict the Hist_Thresh method, as both IWV_Scaled and Decadal_Win methods exhibit a higher number of ARs in the winter season (around 40 ARs) compared to the summer season (around 20-30). This mirrors the observed pattern in the present climate (Figure 3.2, Table 3.1). The contrasting seasonal patterns between these methods and Hist_Thresh underscore the importance of considering different AR detection approaches.

Additionally, IWV_Scaled ARs, on average, have a slightly longer duration compared to those identified using the Decadal_Win method. Further investigation is needed to elucidate the cause of this difference.

3.2.2 Changes in AR Frequency for 2065-2100

Figure 3.7 and Figure 3.8 provide insights into the overall shifts in future AR counts and duration across the Arctic. To understand the regional origins of these changes, an in-depth analysis was conducted of the last 35 years (2065-2100) of the future simulation in comparison to the present climate (1980-2015). This examination aims to examine the spatial variability in AR frequency alterations. Additionally, the section delves into elucidating the contributions of moisture variations to changes in AR frequency in the future climate, drawing comparisons between the Hist_Thresh and IWV_Scaled methods.

In Figure 3.9, the ensemble-mean illustrates absolute changes in AR frequency, while Figure 3.10 presents the ensemble-mean of the relative percentage changes. Figure 3.9a - d delineate the shifts in AR frequency as an absolute frequency change for the Hist_Thresh method. The substantial increase in AR counts and duration culminates in an overall heightened AR frequency across the Arctic throughout all seasons. The central Arctic, witnessing a remarkable ($> 400\%$) increase (Figure 3.10a - d), emerges as a hotspot likely influenced by rising specific humidity following sea-ice loss. However, the Atlantic region, particularly over Greenland during autumn and winter seasons, experiences a much more modest increase, potentially linked to lower sea surface temperatures (SST) in these seasons in response to global warming.

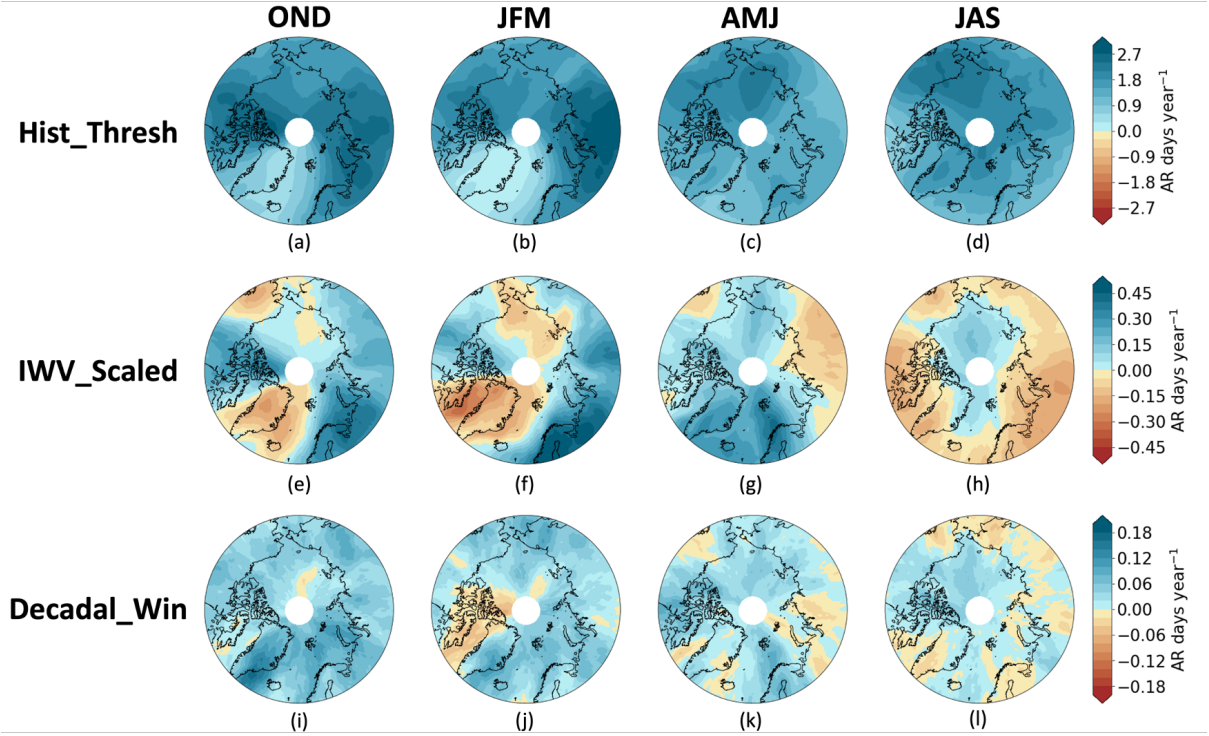

FIGURE 3.9: Ensemble-mean variations in AR frequency from 2065 to 2100 relative to 1980-2014. Panels (a-d) depict the Hist_Thresh method, (e-h) IWV_Scaled method, and (i-l) Decadal_Win method. Changes are expressed in AR-days/year, where blue hues signify increased AR occurrences, while brown hues indicate decreased AR occurrences. Note the difference in scales among the methods.

In contrast to the Hist_Thresh method, both increases and decreases in AR frequency are evident in the other two 'relative relative' methods, IWV_Scaled and Decadal_Win. The IWV_Scaled method reveals diverse changes in AR frequency across seasons (Figure 3.9e - Figure 3.9h), broadly aligning with alterations in mean and extreme meridional velocity at 700 hPa (V700) in future scenarios (Figure 3.11). This suggests that future AR changes in IWV_Scaled are influenced by Arctic circulation shifts.

Using the IWV_Scaled method, during autumn and winter, a substantial reduction in AR frequency is noticeable over Greenland and the North Pacific (Figure 3.9e, Figure 3.9f),

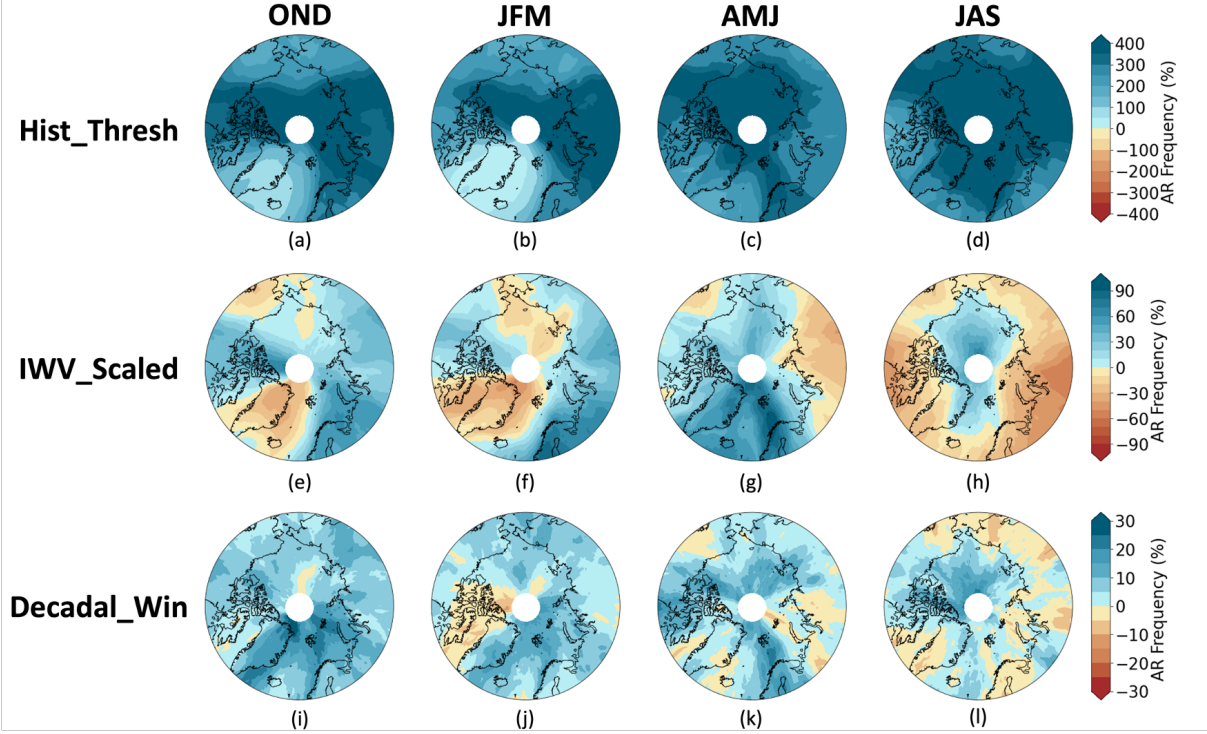

FIGURE 3.10: Same as Figure 3.7 but shows relative percentage change.

while northern Canada and Eurasia experience an increase in AR frequency, with ARs penetrating deeper into the Arctic. Changes in the North Atlantic exhibit complexity using IWV_Scaled with increased AR frequency over Eurasia but declines over the East Greenland region. These changes align well with both mean and extreme V700 changes (Figure 3.11a - f). Conversely, in AMJ, the AR frequency increases by almost 60% (over the Atlantic sector, Canadian sector, and the North Pacific), with more ARs spanning the entire Arctic, excluding Russia (Figure 3.9g). Summer exhibits diminished AR activity across most of the Arctic, especially over land but, increases in the central Arctic region (Figure 3.9h). This shift in AR frequency is likely attributable to ARs penetrating more poleward due to sea ice loss. The future changes in AR frequency broadly align with

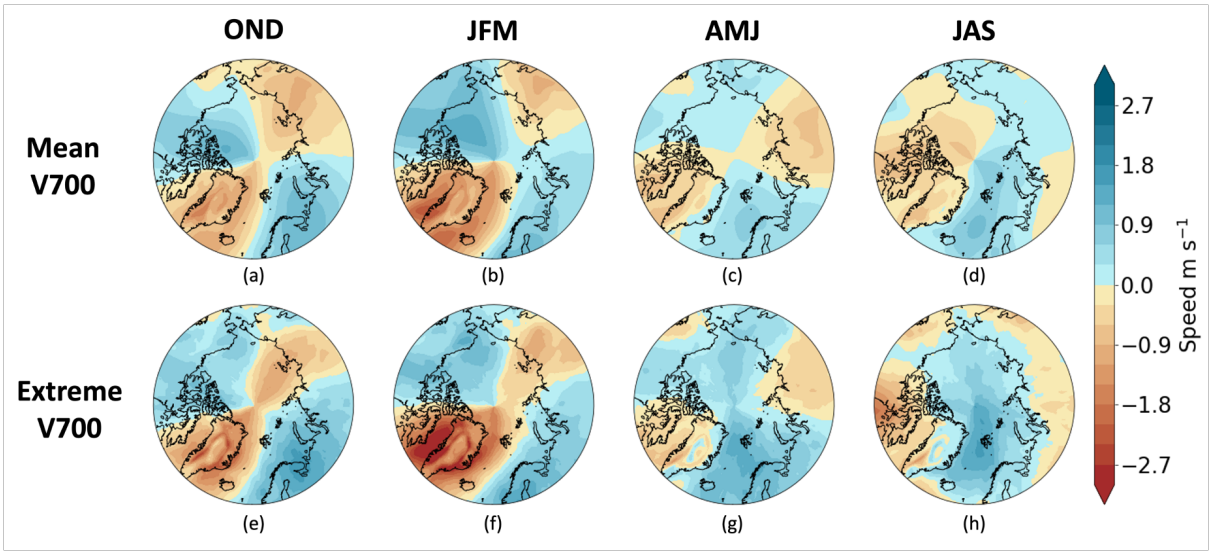

FIGURE 3.11: Ensemble-mean variations in meridional winds at 700 hPa (V700) from 2065 to 2100 relative to 1980-2014. Panels (a-d) depict mean V700, (e-h) extreme winds V700 (98th percentile), where blue hues signify increased Northward winds, while brown hues indicate decreased Northward winds.

alterations in both mean and extreme V700. However, the patterns of mean V700 and extreme V700 during summer are notably different. Although changes in summer AR frequency align with alterations in extreme V700 patterns in the Central Arctic, they do not correspond with mean V700 patterns. Further investigation is necessary to understand the factors causing these divergent wind patterns.

The Decadal_Window method also aims to control for the impact of elevated background moisture, resulting in a modest increase of ARs scattered spatially in the future. In contrast to the IWV_Scaled method, it demonstrates an increase over the Atlantic sector across all seasons. Despite the AR percentage increase being only approximately 20% (Figure 3.10i - l), the subtle increase in AR frequency over Greenland is crucial for studying changes in surface mass balances. For summer, the increase is similar to the

IWV_Scaled method, with more ARs in the central Arctic, but the magnitude of increase is smaller. It is important to note that the results of this method may lack robustness due to a potentially insufficient number of AR cases to discern a clear signal. A larger ensemble size could provide more insights into this aspect.

3.2.3 AR Intensity Changes in Future

Considering the changing frequency of Arctic ARs, understanding alterations in their intensity is crucial due to potential severe impacts. Figure 3.12 shows how AR intensity is projected to change across all seasons in the Arctic. Intensity is defined as the maximum vertically integrated meridional vapor transport (vIVT) of an individual AR, averaged over the season to obtain a mean intensity. Notably, summer Arctic ARs exhibit greater intensity than their winter counterparts. The Hist_Thresh method reveals a slow decline in AR intensity ($p-value < 0.01$) with the changing climate, contrasting sharply with the other two methods, which indicate a notable increase across all seasons (Figure 3.12). Summer shows the largest trends in increasing intensity (IWV_Scaled : 2.628 $kgm^{-1}s^{-1}/year$, Decadal_Win : 1.535 $kgm^{-1}s^{-1}/year$) with winter showing the lowest trend (IWV_Scaled : 0.582 $kgm^{-1}s^{-1}/year$, Decadal_Win : 0.701 $kgm^{-1}s^{-1}/year$).

This discrepancy arises because the Hist_Thresh method encompasses numerous lower-intensity ARs, resulting in an overall lower averaged value per season. Conversely, the substantial increase in AR intensity for IWV_Scaled and Decadal_Win suggests that, despite the heterogeneous changes in AR frequency for these methods, the ARs captured

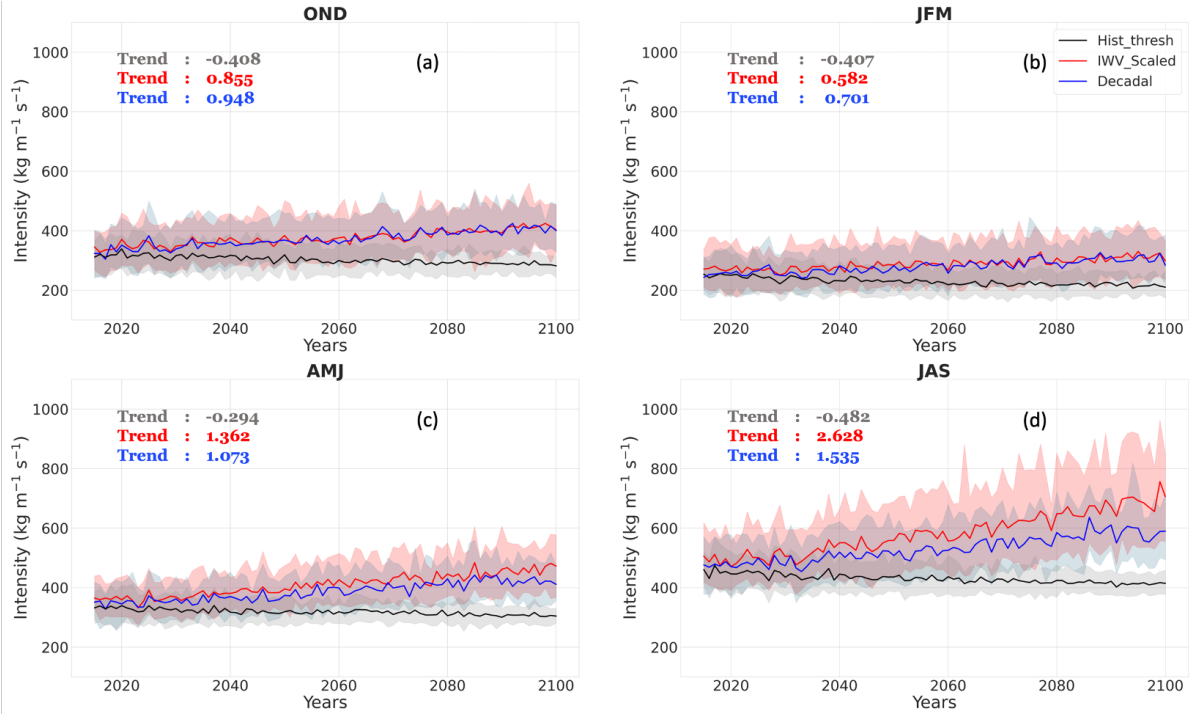

FIGURE 3.12: Average Arctic atmospheric river intensity across seasons: (a) OND, (b) JFM, (c) AMJ, (d) JAS. Solid lines depict the ensemble mean for Hist_Thresh (black), IWV_Scaled (red), and Decadal_Win (blue), while shaded regions in corresponding colors represent the ensemble spread (lower bound : 10th percentile, upper bound : 90th percentile). The trends for each method are shown as increasing intensity ($kgm^{-1}s^{-1}$) / year, with colors corresponding to their respective methods. Statistically non-significant trends are denoted with an asterisk.

become more intense. This heightened intensity is primarily attributed to the increasing moisture content reflected in vIVT. Meridional velocity changes also play a pivotal role; however, it is not uniform across the entire Arctic region (e.g., northward velocity decreases over Greenland in winter Figure 3.11).

3.2.4 Summary

This section demonstrates that Arctic ARs are likely to increase in frequency and become more intense with the changing climate. However, the changes vary regionally, seasonally,

and depending on the method used to detect ARs. Figure 3.13 presents a summary of AR count and intensity changes in the Arctic from 2065 to 2100 across all seasons and four major regions. The findings suggest that the changes in AR frequency are not uniform and are strongly influenced by the method of detection, season, and region. Notably, Arctic ARs exhibit heightened intensity across all regions and methods in the future compared to the present climate (Figure 3.13e - Figure 3.13h). Summer months, attributed to increased moisture availability, experience the most intense ARs compared to other seasons. Methods that incorporate changing climate conditions (IWV_Scaled and Decadal_Win) capture the most intense ARs, leading to higher mean AR intensity compared to the Hist_Thresh method.

Regionally, the Atlantic and Pacific sectors exhibit more intense ARs compared to Eurasia and the Canadian sector. The future changes in AR occurrences demonstrate complexity, driven by background moisture changes, resulting in diverse variations in AR frequency. Once accounted for background moisture changes (IWV_Scaled) a decrease in ARs over summer is observed (Figure 3.13d) as compared to the present climate (1980-2014). While, the Hist_Thresh method reveals the largest increase in frequency during summer, particularly as the Arctic warming makes it easier to meet the statistical threshold for AR detection. Additionally, in winter, the three methods exhibit varied changes in AR occurrences over Greenland (Hist_Thresh and Decadal_Win indicate more ARs, while IWV_Scaled shows fewer ARs), motivating future AR studies in the Greenland region.

Regional and seasonal dependence is evident in changes observed using the IWV_Scaled

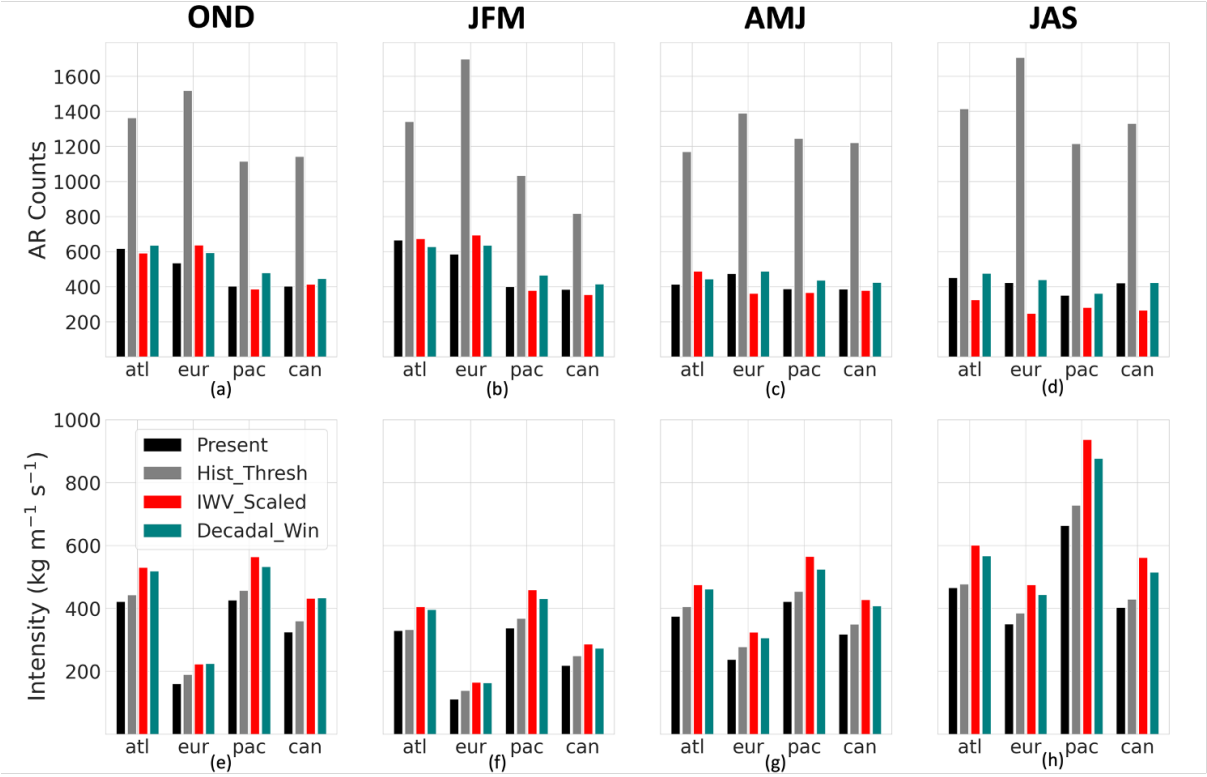

FIGURE 3.13: Regional and seasonal comparison for 2065-2100 of AR counts/year depicted in (a-d) and average AR intensity in (e-h) with present climate (1980-2014) AR conditions presented in black, Hist_Thresh in gray, IWV_Scaled in red, and Decadal_Win in teal. All bars represent the ensemble-mean values.

method, indicating a decrease over Greenland, while Hist_Thresh and Decadal_Win methods show increases. This distinction is crucial, given the significant impacts of ARs over Greenland on ice sheets and regional precipitation. Additionally, the decrease in AR frequency over the Atlantic and Pacific sectors in winter aligns with findings in other studies (Kolbe et al., 2023, Ma et al., 2021).

3.3 Future Arctic ARs and Sea Ice

In this section, we explore the effects of ARs on sea ice in the context of global warming, examining seasonal and spatial variations in impact contingent on the chosen AR detection tool (ARDT). The analysis investigates the overall influence of ARs on sea ice and confronts the challenge of divergent results stemming from varying AR definitions. The central question addressed in this section is :

- **AR Impacts on Sea Ice:** What is the sensitivity of sea ice and its variability to the choice of atmospheric river detection tool (ARDT)?

3.3.1 AR-Induced Sea Ice Loss Calculation

To assess the influence of ARs on sea ice, the variation in sea ice concentration during AR days is examined. However, this method may not accurately reflect the impact of ARs on sea ice, as it might capture only climatological sea ice changes rather than AR-induced changes. To address this, it is essential to subtract the climatological daily rate of sea ice change from the absolute change. However, in a dynamic climate, where sea ice experiences rapid transformations due to climate change, relying on a single value may lead to inaccurate outcomes.

For example, Figure 3.14 illustrates a randomly selected location at 86°N and 15°E, depicting the ensemble-mean, daily rate of change of sea ice concentration ($\Delta\mathrm{SIC}_{xtday}$) for October 28^{th}. The graph reveals significant variations in $\Delta\mathrm{SIC}_{\mathrm{day}}$ from 2015 to 2100.

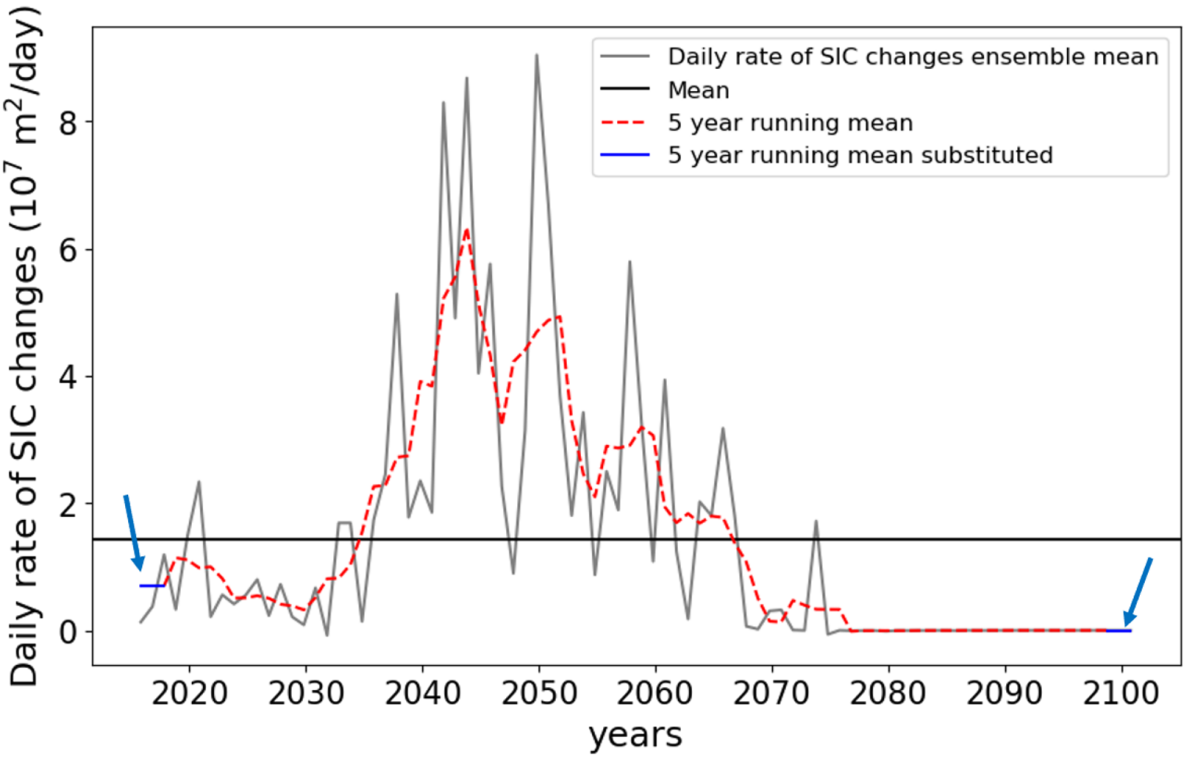

FIGURE 3.14: The ensemble mean daily rate of change in sea-ice concentration (SIC) depicted by the blue line at a random location on October 28^{th}. The black line represents the mean of this change, while the red line illustrates a 5-year running mean of the rate of change of sea-ice concentration. The arrows point towards the data omitted due to running mean and the blue line shows the values used to replace the omitted data. The units for the change in sea-ice concentration are expressed in 10^7 square meters per day.

Initially, the location experiences a small rate of sea ice gain until 2036, after which the rate of sea ice gain increases substantially. By 2075, the location becomes sea ice free, and no further changes in sea ice occur.

When calculating the anomalous change in sea ice during ARs relative to a background rate of change, a potential issue arises. The mean rate of $\Delta\text{SIC}_{\text{day}}$ appears as a constant value (depicted by the black line in the figure). This could lead to errors in the calculation, especially after 2075 when there is no change in sea ice concentration during an AR.

Subtracting the mean ΔSIC_{day} from a zero change may introduce a pseudo gain or loss of sea ice.

To address this, a 5-year running mean of the ΔSIC_{day} is computed (shown by the red dashed line in Figure 3.11). This baseline running mean is then subtracted from the changes in sea ice during AR events amongst individual ensemble members, generating anomalous sea ice change values. Given the utilization of the running mean method, a few data points at the beginning and end of the time-series are omitted, as indicated by arrows in Figure 3.14. These omitted values are replaced with the first and last values of the running mean, as shown by the blue lines in Figure 3.14. This methodology provides a framework for evaluating the nuanced impact of ARs on sea ice over extended time periods. All the results presented in this section use this method.

3.3.2 Total AR-Induced Arctic Sea Ice Changes

Figure 3.12 presents the aggregated sea ice changes during AR events averaged across seasons. The seasonal dynamics of AR-induced sea ice changes exhibit substantial variability, influenced by the frequency and intensity of ARs within each detection method and the overall sea ice conditions during that period. While specific locations may experience either sea ice gain or loss during individual events, an overarching trend of net sea ice loss is observed across the entire Arctic over all seasons, indicating a predominantly negative impact of ARs on future sea ice (i.e. ARs enhance sea ice loss in the future).

The summer season exhibits a relatively smaller sea ice change signal (Figure 3.15d) for

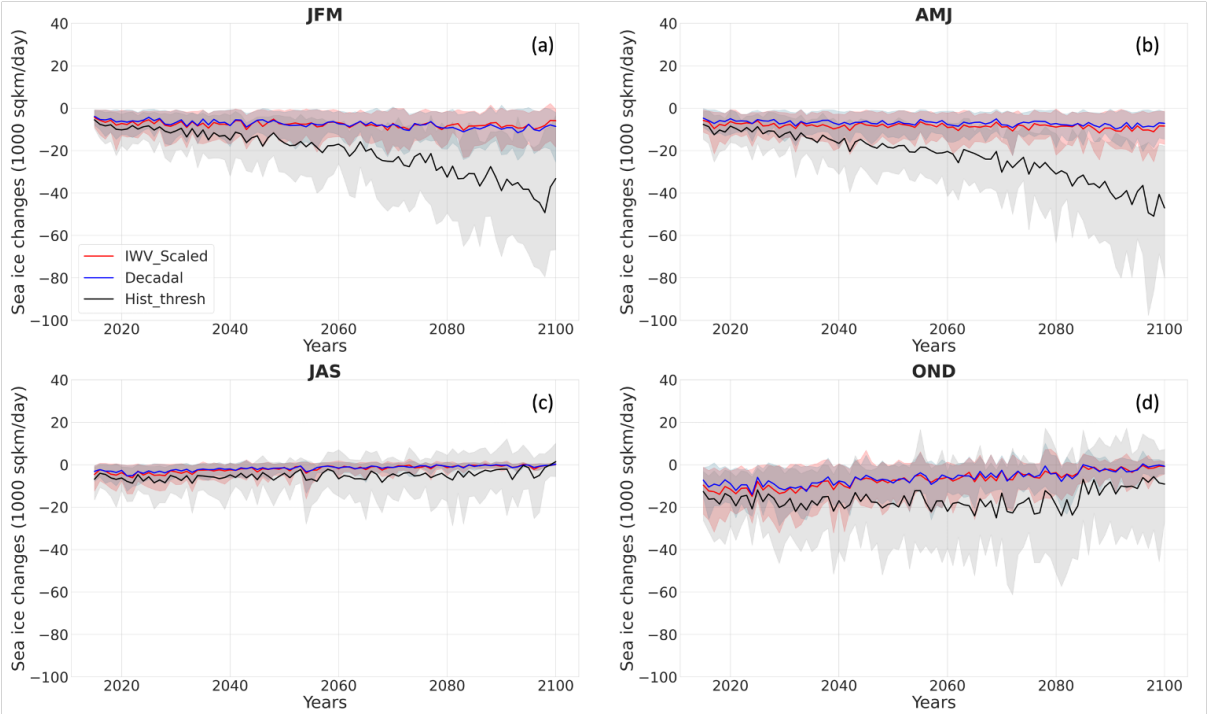

FIGURE 3.15: Average sea-ice changes during atmospheric rivers in the Arctic across seasons: (a) OND, (b) JFM, (c) AMJ, (d) JAS. Solid lines depict the ensemble mean for Hist_Thresh (black), IWV_Scaled (red), and Decadal_Win (blue), while shaded regions in corresponding colors represent the ensemble spread (lower bound : 10th percentile, upper bound : 90th percentile).

several reasons, primarily due to the inherently smaller sea ice extent during this season, reaching its minimum in September. Furthermore, projections indicate that these months may experience sea ice-free conditions in the future, resulting in total sea ice changes approaching zero by the end of the century. In contrast, the winter season displays substantial differences in sea ice changes among different AR detection methods (Figure 3.15b). The Hist_Thresh method, characterized by the highest frequency, demonstrates the largest sea ice changes in the Arctic during winter. However, the sea ice changes associated with ARs detected using the IWV_Scaled and Decadal_Win methods do not exhibit discernible decreasing trends.

The representation of AR-induced sea ice changes becomes increasingly noteworthy in the future as overall sea ice diminishes. The same magnitude of sea ice change would account for a larger percentage of the ice pack, emphasizing the vulnerability of sea ice to extremes. Consequently, as ARs become more intense and frequent, they are poised to hinder winter season sea ice growth. The differences among the different detection methods underscores the importance of methodological choices, particularly the distinction between the Hist_Thresh method and the other two (IWV_Scaled and Decadal_Win methods), in capturing sea ice changes associated with ARs.

3.3.3 Spatial Patterns of AR-Induced Sea Ice changes in 2065-2100

The considerable spatial variation in sea ice changes driven by ARs is prominently illustrated in Figure 3.16, focusing on the alterations expected between 2065-2100. The Hist_Thresh method, as depicted in Figure 3.16, exhibits the most substantial AR-induced sea ice changes across the Arctic, extending beyond the marginal sea ice zone. While the primary impact occurs in the marginal sea ice region, the penetration of ARs deeper into the Arctic, as represented by this method, results in sea ice loss in the central Arctic as well. Notably, during July, August, and September (JAS), sea ice loss is minimal to nonexistent across all methods, aligning with the projected future Arctic's tendency to be ice-free during this period.

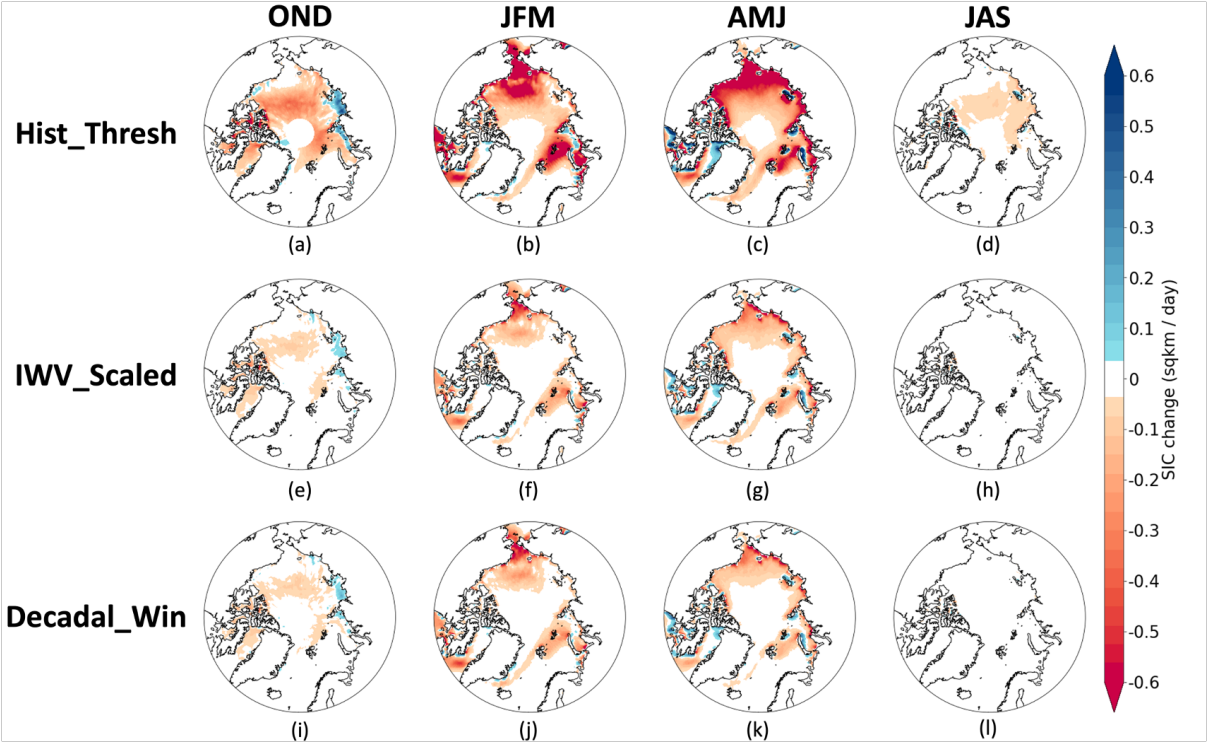

FIGURE 3.16: Ensemble-mean variations in rate of sea ice changes associated with ARs from 2065 to 2100. Panels (a-d) depict the Hist_Thresh method, (e-h) IWV_Scaled method, and (i-l) Decadal_Win method.

Conversely, both IWV_Scaled (Figure 3.16e - h) and Decadal_Win (Figure 3.16i - l) methods exhibit similar patterns in AR influences on sea ice changes. The marginal-sea ice zone experiences enhanced ice loss in all seasons, contingent upon the presence of marginal sea ice extent during that season. The most significant signals are observed over the North Pacific region in winter (JFM), and spring (AMJ), as well as in proximity to Greenland in the Atlantic sector. Instances of sea ice gain, depicted in shades of blue, are attributed to dynamic ice movement pushing towards coastlines. This phenomenon is particularly evident during spring (AMJ), correlating with increased AR frequency over Eurasia (Figure 3.9g, h).

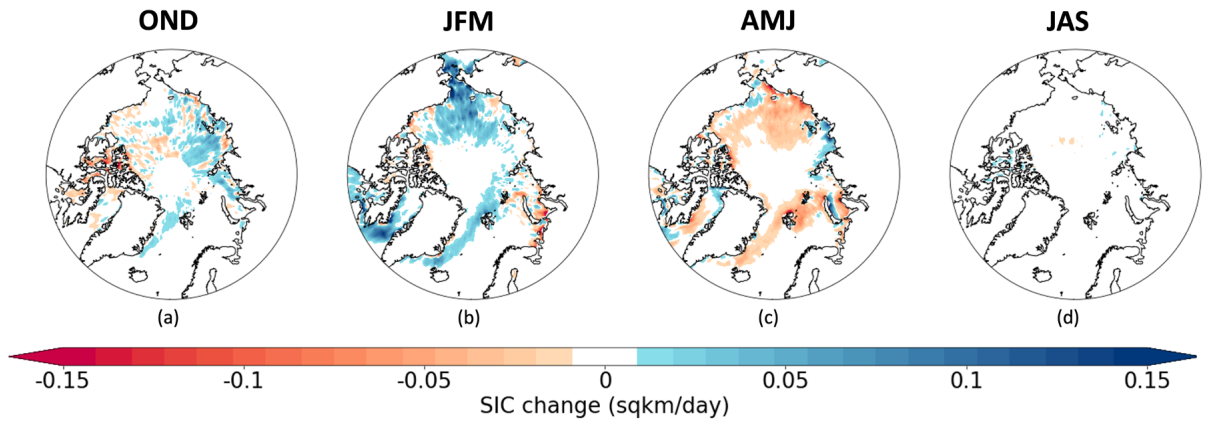

FIGURE 3.17: Difference between AR induced sea-ice changes in IWV_Scaled and Decadal_Win, expressed as IWV_Scaled - Decadal_Win.

Figure 3.17 illustrates the contrast in sea ice changes attributed to ARs between IWV_Scaled and Decadal_Win. Negative values indicate areas where IWV_Scaled depicts greater sea ice loss than Decadal_Win, while blue values signify lesser sea ice loss or gain compared to Decadal_Win. In winter, IWV_Scaled exhibits reduced sea ice loss near the North Pacific and North Atlantic, particularly around Greenland. This discrepancy arises from differences in AR frequency, with IWV_Scaled showing fewer ARs compared to Decadal_Win over these regions. Conversely, in AMJ, IWV_Scaled indicates increased sea ice loss in the central Arctic and greater sea ice gain near coasts compared to Decadal_Win. The higher AR frequency captured by IWV_Scaled across most of the Arctic intensifies the sea ice loss signal, although the Laptev Sea experiences sea ice gain, potentially due to fewer ARs in that region compared to Decadal_Win.

3.3.4 Summary

In summary, the future climate shows increased sea ice loss, particularly during winter and spring. As overall sea ice diminishes, the AR-induced sea ice loss decreases, reaching zero in summer and fall. However, ARs during winter and spring induce a net negative impact on sea ice. The AR-induced sea ice loss during these seasons amplifies in response to warming climate, notably pronounced in Hist_Thresh method. The specific regions and extent of AR-associated sea ice changes are strongly influenced by the choice of AR detection method. While sea ice changes are typically concentrated around the marginal sea ice, our findings reveal that variations in the magnitude and the sign of AR-induced sea ice change are contingent on the AR detection method.

Chapter 4

Discussion

This study builds upon previous research that has highlighted the increasing frequency of Arctic ARs in warmer climates (Kolbe et al., 2023, Ma et al., 2021). Unlike earlier studies focusing on specific seasons or annual changes, this research pioneers a comprehensive exploration of seasonal variations in Arctic ARs, employing three distinct AR detection methods to shed light on the uncertainties associated with methodological choices. This study also delves into the roles of thermodynamics and dynamics in shaping AR characteristics. Furthermore, the primary findings obtained here from a climate model subjected to transient greenhouse gas forcing, aligns with previous studies that were run for a shorter time and with forced atmospheric or sea-ice conditions. This study also underscores the future impact of ARs on sea-ice, serving as a catalyst for further investigations. Moreover, recognizing the distinction between ARs and extratropical cyclones

or moisture intrusion events does not suggest their complete separation; instead, it offers additional insights that complement existing studies on cyclones and heatwaves.

This study emphasizes the influence moisture on future Arctic ARs by comparing the Hist_Thresh, IWV_Scaled, and Decadal_Win methods. However, emphasis is placed on the IWV_Scaled method for a more in-depth understanding, as its changes can be predominantly elucidated by alterations in circulation patterns (Figure 3.9 and Figure 3.11). Our findings indicate that the projected rise in AR frequency is primarily caused by increasing moisture, potentially due to the Clausius-Clapeyron effect or other factors like moisture convergence. The observed alterations in AR frequency using IWV_Scaled method, align with the outcomes of previous studies by Ma et al. (2021) and Kolbe et al. (2023) such as the decrease in AR frequency over the North Atlantic, North Pacific, and near Greenland. Although this study doesn't delve into detailed jet stream changes, the shifts in ARs using IWV_Scaled method may be influenced by the future climate's alterations in the jet stream position (Kolbe et al., 2023, Ma et al., 2021, Sousa et al., 2020, Zhang et al., 2021). These changes in the jet stream appear to result from a complex interplay between factors such as Arctic Amplification and the warming upper tropical troposphere (for example, Deser et al. (2010, 2015), Screen et al. (2013)). Liu and Barnes (2015) have also shown that strong moisture intrusion events are significantly influenced by Rossby wave breaking. In addition, the seasonal changes in poleward moisture transport are mainly influenced by the background moisture gradient, a factor relevant to this study as well.

Mattingly et al. (2018, 2020, 2023) demonstrated the substantial influence of ARs on the Greenland ice sheet, primarily by modulating the total surface mass balance through radiative imbalance and the foehn winds linked to ARs. These studies show the significance of accurately capturing ARs in future climate scenarios to comprehend their impact on Greenland. However, our findings reveal disparate changes in AR frequency over Greenland based on different detection methods (Figure 3.9). While ice sheets and sea ice are indifferent to the definition of extremes in a changing climate, attributing losses to ARs remains a subject for further investigation due to uncertainties in defining ARs in the future. Therefore, the development of an improved AR identification method, moving beyond statistical threshold approaches, becomes imperative.

Moreover, this work highlights the impact of varied AR definitions in a changing climate, revealing the potential for diverse outcomes. Several studies like Zhang et al. (2021) and Zhao (2020) examining global ARs in a warming climate have often overlooked shifts in detection thresholds, aligning closely with results akin to the Hist_Thresh method. In the Arctic, this disparity is more pronounced, ranging from an approximately 400% increase to a decrease in future AR frequency across seasons and regions. This underscores the need for addressing such uncertainties in other studies as well.

Moreover, as indicated by Zhang et al. (2023) and Li et al. (2022), winter ARs consistently promote sea ice melting leading to a smaller winter sea ice extent. This trend persists as the Arctic undergoes warming in the future, rendering sea ice more susceptible to ARs and leading to a greater proportion of sea-ice loss, particularly evident under the

Hist_Thresh method. The AR induced sea-ice changes in spring follow a similar pattern to those in winter. This is a significant aspect to investigate, given previous research indicating that AR-like structures in spring can trigger the onset of sea-ice melt (Yang and Magnusdottir, 2017). Additionally, while an overall net negative impact on sea ice prevails, it is noteworthy that certain ensemble members yield a net positive sea ice change. The summer months, marked by reduced initial sea-ice extent, experience relatively minor sea-ice changes. This is attributed to the balancing effect of AR-induced changes, resulting in a modest net negative impact. Understanding these nuanced interactions is crucial for a comprehensive assessment of AR influences on Arctic sea ice.

There are few limitations of this study. For example, the evaluation of CESM2 against ERA5 indicates a tendency for CESM2 to overestimate AR frequency and intensity throughout all seasons. These discrepancies may stem from CESM2's relatively smaller sea ice volume and thickness compared to observed values (DeRepentigny et al., 2020, DuVivier et al., 2020) and warmer surface across the Arctic (McIlhattan et al., 2020). This might suggest a potential increase in evaporation and specific humidity in the Arctic and potentially providing more energy for ARs. However, further investigation is needed for confirmation. Additionally, CESM2 tends to produce more liquid-containing clouds (LCC) and increased rainfall in the Arctic (McIlhattan et al., 2020). As ARs influence both clouds and precipitation, biases in AR frequency and intensity could contribute to biases in LCC and rainfall.

Despite CESM2's ability to capture extratropical cyclones well (Simpson et al., 2020),

its 1-degree spatial resolution may not be optimal for studying extreme events like ARs (Collow et al., 2022). Moreover, the position and magnitude of ARs are influenced by the jet stream and blocking, and while CESM2 compares favorably to other CMIP6 models, it exhibits a bias in estimating jet stream location and speed. For example, the jet stream is faster over the Pacific and Atlantic and slightly too far north in the Atlantic (Simpson et al., 2020). Additionally, this study assumes that CESM2's biases in the present climate remain consistent in the future, which may not hold true.

Another limitation of this study lies in maintaining the 98^{th} percentile threshold on vertically integrated meridional integrated vapor transport (vIVT). This limitation confines the results to meridionally oriented ARs. While this approach effectively captures polar ARs (Maclennan et al., 2022, Wille et al., 2019, 2021), ARs with stronger zonal velocity and weaker meridional velocity may not be adequately captured, along with their associated impacts. Moreover, unlike other studies that have demonstrated increased AR occurrences in present and future climate by lowering the percentile threshold (e.g., 85th percentile, 90th percentile), with spatial patterns and trends remaining consistent (Kolbe et al., 2023, Zhang et al., 2023), this study did not investigate this aspect. Another limitation shared with similar studies is the ongoing debate surrounding the definition of atmospheric rivers. Numerous detection algorithms in the literature propose various statistical criteria, often relying on percentile thresholds, resulting in varied outcomes across different regions. Consequently, there is a need for a more universal and standardized approach to identify this atmospheric phenomenon. Considering that ARs are linked to robust polar moisture transport, an alternative approach could involve identification

based on poleward moisture transport associated with transient eddies in the atmosphere (Mahesh et al., 2023). However, this is a relatively novel method and subject to ongoing debate within the scientific community. Addressing these considerations will contribute to refining the understanding and consistent identification of atmospheric rivers.

Chapter 5

Conclusion and Future Work

In summary, the evaluation of CESM2 against ERA5 (Section 3.1) reveals that CESM2 generally performs well in depicting Arctic ARs in the present climate (1980-2015). Section 3.2 shows that Arctic atmospheric rivers generally become more frequent and intense with ongoing greenhouse gas warming. However, the specifics of future AR changes vary greatly according to the chosen detection method, showcasing seasonal and regional differences and emphasizing the significance of such comparison. Finally, Section 3.3 highlights the net impact of ARs on sea-ice, revealing that ARs consistently promote sea-ice loss. However, the magnitude and location of these losses are notably influenced by the method used to define ARs in a changing climate. The study yields the following key findings:

1. CESM2 realistically simulates Arctic ARs, demonstrating suitability for future AR investigations, despite some biases compared to ERA5.

2. Arctic ARs exhibit increased frequency and intensity in the future climate, but this rise is heavily influenced by the chosen AR definition, as detailed in the Chapter 2.

3. The increased AR occurrences in the future is primarily driven by moisture changes.

4. Circulation changes result in fewer ARs over Greenland, the North Atlantic, and the North Pacific during winter, along with an overall decrease in summer and a slight increase in the central Arctic. Spring experiences the most substantial increase in AR frequency.

5. The Pacific sector demonstrates the most substantial increase in AR intensity across all seasons, particularly in summer.

6. AR-induced sea-ice changes consistently indicate a net loss, with the highest impact observed in winter and spring.

7. Changes in AR impact on sea-ice are notably sensitive to the chosen AR definition in a warmer climate.

The findings of this study pave the way for future research inquiries, particularly in the detailed investigation of the factors contributing to sea ice changes induced by ARs. A comprehensive approach involves decomposing these changes into thermodynamic and dynamic components, followed by a heat budget analysis to unravel the respective roles of the atmosphere and ocean in AR-induced sea-ice alterations.

Studying Arctic ARs provides valuable insights into poleward moisture transport and its potential variations under future climatic conditions, driven by changes in temperature and moisture gradients between the tropics and poles. This line of inquiry aims to establish a more physically grounded definition of ARs, moving beyond purely statistical considerations.

Additionally, ARs are linked to increased cloudiness and precipitation. Future investigations could delve into understanding how ARs influence different cloud types and their heights in the Arctic, as well as how precipitation regimes are evolving. Exploring whether ARs contribute more to rainfall or snowfall in both present and future climates is a crucial aspect of this research. Another avenue worth exploring involves conducting a moisture tracking experiment. This would provide a broader perspective on the import of moisture and shed light on how the genesis of moisture changes with a warming climate. This, in turn, would contribute valuable insights to the various topics described above.

In conclusion, this investigation into Arctic ARs within the context of climate change has unveiled intriguing patterns and impacts, yet much remains unexplored. This avenue not only provides insights into the present but also for the future, contributing to a better understanding of Arctic climate dynamics.

May the Moisture Flux be with you

Bibliography

Allan, R. P., C. Liu, M. Zahn, D. A. Lavers, E. Koukouvagias, and A. Bodas-Salcedo, 2014: Physically Consistent Responses of the Global Atmospheric Hydrological Cycle in Models and Observations. *Surveys in Geophysics*, **35 (3)**, 533–552, doi:10.1007/s10712-012-9213-z, URL https://doi.org/10.1007/s10712-012-9213-z.

Aue, L., and A. Rinke, 2023: Cyclone Impacts on Sea Ice Concentration in the Atlantic Arctic Ocean: Annual Cycle and Recent Changes. *Geophysical Research Letters*, **50 (17)**, e2023GL104 657, doi:10.1029/2023GL104657, URL https://onlinelibrary.wiley.com/doi/abs/10.1029/2023GL104657, _eprint: https://onlinelibrary.wiley.com/doi/pdf/10.1029/2023GL104657.

Bachand, C. L., and J. E. Walsh, 2022: Extreme Precipitation Events in Alaska: Historical Trends and Projected Changes. *Atmosphere*, **13 (3)**, 388, doi:10.3390/atmos13030388, URL https://www.mdpi.com/2073-4433/13/3/388, number: 3 Publisher: Multidisciplinary Digital Publishing Institute.

Clancy, R., C. M. Bitz, E. Blanchard-Wrigglesworth, M. C. McGraw, and S. M. Cavallo, 2022: A cyclone-centered perspective on the drivers of asymmetric patterns in

the atmosphere and sea ice during Arctic cyclones. *Journal of Climate*, **-1 (aop)**, 1–47, doi:10.1175/JCLI-D-21-0093.1, URL https://journals.ametsoc.org/view/journals/clim/aop/JCLI-D-21-0093.1/JCLI-D-21-0093.1.xml, publisher: American Meteorological Society Section: Journal of Climate.

Collow, A. B. M., and Coauthors, 2022: An overview of artmip's tier 2 reanalysis intercomparison: Uncertainty in the detection of atmospheric rivers and their associated precipitation. *Journal of Geophysical Research: Atmospheres*, **127 (8)**, e2021JD036 155, doi:https://doi.org/10.1029/2021JD036155, URL https://agupubs.onlinelibrary.wiley.com/doi/abs/10.1029/2021JD036155, e2021JD036155 2021JD036155, https://agupubs.onlinelibrary.wiley.com/doi/pdf/10.1029/2021JD036155.

Corringham, T. W., F. M. Ralph, A. Gershunov, D. R. Cayan, and C. A. Talbot, 2019: Atmospheric rivers drive flood damages in the western United States. *Science Advances*, **5 (12)**, eaax4631, doi:10.1126/sciadv.aax4631, URL https://www.science.org/doi/10.1126/sciadv.aax4631, publisher: American Association for the Advancement of Science.

Danabasoglu, G., and Coauthors, 2020: The Community Earth System Model Version 2 (CESM2). *Journal of Advances in Modeling Earth Systems*, **12 (2)**, e2019MS001 916, doi:10.1029/2019MS001916, URL https://onlinelibrary.wiley.com/doi/abs/10.1029/2019MS001916, _eprint: https://onlinelibrary.wiley.com/doi/pdf/10.1029/2019MS001916.

DeRepentigny, P., A. Jahn, M. M. Holland, and A. Smith, 2020: Arctic Sea Ice in Two Configurations of the CESM2 During the 20th and 21st Centuries. *Journal of Geophysical Research: Oceans*, **125 (9)**, e2020JC016 133, doi:10.1029/2020JC016133, URL https://onlinelibrary.wiley.com/doi/abs/10.1029/2020JC016133, _eprint: https://onlinelibrary.wiley.com/doi/pdf/10.1029/2020JC016133.

Deser, C., R. Tomas, M. Alexander, and D. Lawrence, 2010: The Seasonal Atmospheric Response to Projected Arctic Sea Ice Loss in the Late Twenty-First Century. *Journal of Climate*, **23 (2)**, 333–351, doi:10.1175/2009JCLI3053.1, URL https://journals.ametsoc.org/view/journals/clim/23/2/2009jcli3053.1.xml, publisher: American Meteorological Society Section: Journal of Climate.

Deser, C., R. A. Tomas, and L. Sun, 2015: The Role of Ocean–Atmosphere Coupling in the Zonal-Mean Atmospheric Response to Arctic Sea Ice Loss. *Journal of Climate*, **28 (6)**, 2168–2186, doi:10.1175/JCLI-D-14-00325.1, URL https://journals.ametsoc.org/view/journals/clim/28/6/jcli-d-14-00325.1.xml, publisher: American Meteorological Society Section: Journal of Climate.

DuVivier, A. K., M. M. Holland, J. E. Kay, S. Tilmes, A. Gettelman, and D. A. Bailey, 2020: Arctic and Antarctic Sea Ice Mean State in the Community Earth System Model Version 2 and the Influence of Atmospheric Chemistry. *Journal of Geophysical Research: Oceans*, **125 (8)**, e2019JC015 934, doi:10.1029/2019JC015934, URL https://onlinelibrary.wiley.com/doi/abs/10.1029/2019JC015934, _eprint: https://onlinelibrary.wiley.com/doi/pdf/10.1029/2019JC015934.

Espinoza, V., D. E. Waliser, B. Guan, D. A. Lavers, and F. M. Ralph, 2018: Global Analysis of Climate Change Projection Effects on Atmospheric Rivers. *Geophysical Research Letters*, **45 (9)**, 4299–4308, doi:10.1029/2017GL076968, URL https://onlinelibrary.wiley.com/doi/abs/10.1029/2017GL076968, _eprint: https://onlinelibrary.wiley.com/doi/pdf/10.1029/2017GL076968.

Francis, D., K. S. Mattingly, M. Temimi, R. Massom, and P. Heil, 2020: On the crucial role of atmospheric rivers in the two major Weddell Polynya events in 1973 and 2017 in Antarctica. *Science Advances*, **6 (46)**, eabc2695, doi:10.1126/sciadv.abc2695, URL https://www.science.org/doi/10.1126/sciadv.abc2695, publisher: American Association for the Advancement of Science.

Francis, J. A., S. J. Vavrus, and J. Cohen, 2017: Amplified Arctic warming and mid-latitude weather: new perspectives on emerging connections. *WIREs Climate Change*, **8 (5)**, e474, doi:10.1002/wcc.474, URL https://onlinelibrary.wiley.com/doi/abs/10.1002/wcc.474, _eprint: https://onlinelibrary.wiley.com/doi/pdf/10.1002/wcc.474.

Gao, Y., J. Lu, and L. R. Leung, 2016: Uncertainties in Projecting Future Changes in Atmospheric Rivers and Their Impacts on Heavy Precipitation over Europe. *Journal of Climate*, **29 (18)**, 6711–6726, doi:10.1175/JCLI-D-16-0088.1, URL https://journals.ametsoc.org/view/journals/clim/29/18/jcli-d-16-0088.1.xml, publisher: American Meteorological Society Section: Journal of Climate.

Gao, Y., J. Lu, L. R. Leung, Q. Yang, S. Hagos, and Y. Qian, 2015: Dynamical and thermodynamical modulations on future changes of landfalling atmospheric rivers over western North America. *Geophysical Research Letters*, **42 (17)**, 7179–7186, doi:10.1002/2015GL065435, URL https://onlinelibrary.wiley.com/doi/abs/10.1002/2015GL065435, _eprint: https://onlinelibrary.wiley.com/doi/pdf/10.1002/2015GL065435.

Gimeno, L., M. Vázquez, R. Nieto, and R. M. Trigo, 2015: Atmospheric moisture transport: the bridge between ocean evaporation and Arctic ice melting. *Earth System Dynamics*, **6 (2)**, 583–589, doi:10.5194/esd-6-583-2015, URL https://esd.copernicus.org/articles/6/583/2015/, publisher: Copernicus GmbH.

Graham, R. M., L. Cohen, A. A. Petty, L. N. Boisvert, A. Rinke, S. R. Hudson, M. Nicolaus, and M. A. Granskog, 2017a: Increasing frequency and duration of Arctic winter warming events. *Geophysical Research Letters*, **44 (13)**, 6974–6983, doi:10.1002/2017GL073395, URL https://onlinelibrary.wiley.com/doi/abs/10.1002/2017GL073395, _eprint: https://onlinelibrary.wiley.com/doi/pdf/10.1002/2017GL073395.

Graham, R. M., L. Cohen, A. A. Petty, L. N. Boisvert, A. Rinke, S. R. Hudson, M. Nicolaus, and M. A. Granskog, 2017b: Increasing frequency and duration of Arctic winter warming events. *Geophysical Research Letters*, **44 (13)**, 6974–6983, doi:10.1002/2017GL073395, URL https://onlinelibrary.wiley.com/doi/abs/10.1002/2017GL073395, _eprint: https://onlinelibrary.wiley.com/doi/pdf/10.1002/2017GL073395.

Guan, B., and D. E. Waliser, 2015: Detection of atmospheric rivers: Evaluation and application of an algorithm for global studies. *Journal of Geophysical Research: Atmospheres*, **120 (24)**, 12 514–12 535, doi:10.1002/2015JD024257, URL https://onlinelibrary.wiley.com/doi/abs/10.1002/2015JD024257, _eprint: https://onlinelibrary.wiley.com/doi/pdf/10.1002/2015JD024257.

Held, I. M., and B. J. Soden, 2006: Robust responses of the hydrological cycle to global warming. *Journal of Climate*, **19 (21)**, 5686 – 5699, doi:https://doi.org/10.1175/JCLI3990.1, URL https://journals.ametsoc.org/view/journals/clim/19/21/jcli3990.1.xml.

Hersbach, H., and Coauthors, 2020: The ERA5 global reanalysis. *Quarterly Journal of the Royal Meteorological Society*, **146 (730)**, 1999–2049, doi:10.1002/qj.3803, URL https://onlinelibrary.wiley.com/doi/abs/10.1002/qj.3803, _eprint: https://onlinelibrary.wiley.com/doi/pdf/10.1002/qj.3803.

Kolbe, M., J. P. J. Sonnemans, R. Bintanja, E. C. van der Linden, K. van der Wiel, K. Whan, and I. Benedict, 2023: Impact of atmospheric rivers on future poleward moisture transport and arctic climate in ec-earth2. *Journal of Geophysical Research: Atmospheres*, **128 (18)**, e2023JD038 926, doi:https://doi.org/10.1029/2023JD038926, URL https://agupubs.onlinelibrary.wiley.com/doi/abs/10.1029/2023JD038926, e2023JD038926 2023JD038926, https://agupubs.onlinelibrary.wiley.com/doi/pdf/10.1029/2023JD038926.

Li, L., F. Cannon, M. R. Mazloff, A. C. Subramanian, A. M. Wilson, and F. M. Ralph, 2022: Impact of atmospheric rivers on arctic sea ice variations. *EGUsphere*, **2022**, 1–21, doi:10.5194/egusphere-2022-36, URL https://egusphere.copernicus.org/preprints/2022/egusphere-2022-36/.

Liu, C., and E. A. Barnes, 2015: Extreme moisture transport into the arctic linked to rossby wave breaking. *Journal of Geophysical Research: Atmospheres*, **120 (9)**, 3774–3788, doi:https://doi.org/10.1002/2014JD022796, URL https://agupubs.onlinelibrary.wiley.com/doi/abs/10.1002/2014JD022796, https://agupubs.onlinelibrary.wiley.com/doi/pdf/10.1002/2014JD022796.

Ma, W., G. Chen, Y. Peings, and N. Alviz, 2021: Atmospheric River Response to Arctic Sea Ice Loss in the Polar Amplification Model Intercomparison Project. *Geophysical Research Letters*, **48 (20)**, e2021GL094 883, doi:https://doi.org/10.1029/2021GL094883, URL https://agupubs.onlinelibrary.wiley.com/doi/abs/10.1029/2021GL094883, _eprint: https://agupubs.onlinelibrary.wiley.com/doi/pdf/10.1029/2021GL094883.

Maclennan, M. L., J. T. M. Lenaerts, C. Shields, and J. D. Wille, 2022: Contribution of atmospheric rivers to antarctic precipitation. *Geophysical Research Letters*, **49 (18)**, e2022GL100 585, doi:https://doi.org/10.1029/2022GL100585, URL https://agupubs.onlinelibrary.wiley.com/doi/abs/10.1029/2022GL100585, e2022GL100585 2022GL100585, https://agupubs.onlinelibrary.wiley.com/doi/pdf/10.1029/2022GL100585.

Mahesh, A., T. O'Brien, B. Loring, A. Elbashandy, W. Boos, and W. Collins, 2023: Identifying Atmospheric Rivers and their Poleward Latent Heat Transport with Generalizable Neural Networks: ARCNNv1. *EGUsphere*, 1–36, doi:10.5194/egusphere-2023-763, URL https://egusphere.copernicus.org/preprints/2023/egusphere-2023-763/, publisher: Copernicus GmbH.

Mattingly, K. S., T. L. Mote, and X. Fettweis, 2018: Atmospheric River Impacts on Greenland Ice Sheet Surface Mass Balance. *Journal of Geophysical Research: Atmospheres*, **123 (16)**, 8538–8560, doi:10.1029/2018JD028714, URL https://onlinelibrary.wiley.com/doi/abs/10.1029/2018JD028714, _eprint: https://onlinelibrary.wiley.com/doi/pdf/10.1029/2018JD028714.

Mattingly, K. S., T. L. Mote, X. Fettweis, D. van As, K. V. Tricht, S. Lhermitte, C. Pettersen, and R. S. Fausto, 2020: Strong summer atmospheric rivers trigger greenland ice sheet melt through spatially varying surface energy balance and cloud regimes. *Journal of Climate*, **33 (16)**, 6809 – 6832, doi:https://doi.org/10.1175/JCLI-D-19-0835.1, URL https://journals.ametsoc.org/view/journals/clim/33/16/jcliD190835.xml.

Mattingly, K. S., J. V. Turton, J. D. Wille, B. Noël, X. Fettweis, K. Rennermalm, and T. L. Mote, 2023: Increasing extreme melt in northeast Greenland linked to foehn winds and atmospheric rivers. *Nature Communications*, **14 (1)**, 1743, doi:10.1038/s41467-023-37434-8, URL https://www.nature.com/articles/s41467-023-37434-8, number: 1 Publisher: Nature Publishing Group.

McIlhattan, E. A., J. E. Kay, and T. S. L'Ecuyer, 2020: Arctic clouds and precipitation in the community earth system model version 2. *Journal of Geophysical Research: Atmospheres*, **125 (22)**, e2020JD032 521, doi:https://doi.org/10.1029/2020JD032521, URL https://agupubs.onlinelibrary.wiley.com/doi/abs/10.1029/2020JD032521, e2020JD032521 10.1029/2020JD032521, https://agupubs.onlinelibrary.wiley.com/doi/pdf/10.1029/2020JD032521.

Nash, D., D. Waliser, B. Guan, H. Ye, and F. M. Ralph, 2018: The role of atmospheric rivers in extratropical and polar hydroclimate. *Journal of Geophysical Research: Atmospheres*, **123 (13)**, 6804–6821, doi:https://doi.org/10.1029/2017JD028130, URL https://agupubs.onlinelibrary.wiley.com/doi/abs/10.1029/2017JD028130, https://agupubs.onlinelibrary.wiley.com/doi/pdf/10.1029/2017JD028130.

O'Brien, T. A., and Coauthors, 2022: Increases in Future AR Count and Size: Overview of the ARTMIP Tier 2 CMIP5/6 Experiment. *Journal of Geophysical Research: Atmospheres*, **127 (6)**, e2021JD036 013, doi:10.1029/2021JD036013, URL https://onlinelibrary.wiley.com/doi/abs/10.1029/2021JD036013, _eprint: https://onlinelibrary.wiley.com/doi/pdf/10.1029/2021JD036013.

Paltan, H., D. Waliser, W. H. Lim, B. Guan, D. Yamazaki, R. Pant, and S. Dadson, 2017: Global Floods and Water Availability Driven by Atmospheric Rivers. *Geophysical Research Letters*, **44 (20)**, 10,387–10,395, doi:10.1002/2017GL074882, URL https://onlinelibrary.wiley.com/doi/abs/10.1002/2017GL074882, _eprint: https://onlinelibrary.wiley.com/doi/pdf/10.1002/2017GL074882.

Pan, M., and M. Lu, 2020: East Asia Atmospheric River catalog: Annual Cycle, Transition Mechanism, and Precipitation. *Geophysical Research Letters*, **47 (15)**, e2020GL089 477, doi:10.1029/2020GL089477, URL https://onlinelibrary.wiley.com/doi/abs/10.1029/2020GL089477, _eprint: https://onlinelibrary.wiley.com/doi/pdf/10.1029/2020GL089477.

Papritz, L., D. Hauswirth, and K. Hartmuth, 2022: Moisture origin, transport pathways, and driving processes of intense wintertime moisture transport into the Arctic. *Weather and Climate Dynamics*, **3 (1)**, 1–20, doi:10.5194/wcd-3-1-2022, URL https://wcd.copernicus.org/articles/3/1/2022/, publisher: Copernicus GmbH.

Payne, A. E., and G. Magnusdottir, 2015: An evaluation of atmospheric rivers over the North Pacific in CMIP5 and their response to warming under RCP 8.5. *Journal of Geophysical Research: Atmospheres*, **120 (21)**, 11,173–11,190, doi:10.1002/2015JD023586, URL https://onlinelibrary.wiley.com/doi/abs/10.1002/2015JD023586, _eprint: https://onlinelibrary.wiley.com/doi/pdf/10.1002/2015JD023586.

Prince, H. D., N. J. Cullen, P. B. Gibson, J. Conway, and D. G. Kingston, 2021: A Climatology of Atmospheric Rivers in New Zealand. *Journal of Climate*, **34 (11)**, 4383–4402, doi:10.1175/JCLI-D-20-0664.1, URL https://journals.ametsoc.org/view/journals/clim/34/11/JCLI-D-20-0664.1.xml, publisher: American Meteorological Society Section: Journal of Climate.

Ralph, F. M., M. D. Dettinger, M. M. Cairns, T. J. Galarneau, and J. Eylander, 2018: Defining "atmospheric river": How the glossary of meteorology helped resolve a debate.

Bulletin of the American Meteorological Society, **99 (4)**, 837 – 839, doi:https://doi.org/10.1175/BAMS-D-17-0157.1, URL https://journals.ametsoc.org/view/journals/bams/99/4/bams-d-17-0157.1.xml.

Reid, K. J., A. D. King, T. P. Lane, and D. Hudson, 2022: Tropical, Subtropical, and Extratropical Atmospheric Rivers in the Australian Region. *Journal of Climate*, **35 (9)**, 2697–2708, doi:10.1175/JCLI-D-21-0606.1, URL https://journals.ametsoc.org/view/journals/clim/35/9/JCLI-D-21-0606.1.xml, publisher: American Meteorological Society Section: Journal of Climate.

Reid, K. J., S. M. Rosier, L. J. Harrington, A. D. King, and T. P. Lane, 2021: Extreme rainfall in New Zealand and its association with Atmospheric Rivers. *Environmental Research Letters*, **16 (4)**, 044 012, doi:10.1088/1748-9326/abeae0, URL https://dx.doi.org/10.1088/1748-9326/abeae0, publisher: IOP Publishing.

Rinke, A., M. Maturilli, R. M. Graham, H. Matthes, D. Handorf, L. Cohen, S. R. Hudson, and J. C. Moore, 2017: Extreme cyclone events in the Arctic: Wintertime variability and trends. *Environmental Research Letters*, **12 (9)**, 094 006, doi:10.1088/1748-9326/aa7def, URL https://dx.doi.org/10.1088/1748-9326/aa7def, publisher: IOP Publishing.

Rodgers, K. B., and Coauthors, 2021: Ubiquity of human-induced changes in climate variability. *Earth System Dynamics*, **12 (4)**, 1393–1411, doi:10.5194/esd-12-1393-2021, URL https://esd.copernicus.org/articles/12/1393/2021/, publisher: Copernicus GmbH.

Rutz, J. J., and Coauthors, 2019: The Atmospheric River Tracking Method Intercomparison Project (ARTMIP): Quantifying Uncertainties in Atmospheric River Climatology. *Journal of Geophysical Research: Atmospheres*, **124 (24)**, 13 777–13 802, doi:10.1029/2019JD030936, URL https://onlinelibrary.wiley.com/doi/abs/10.1029/2019JD030936, _eprint: https://onlinelibrary.wiley.com/doi/pdf/10.1029/2019JD030936.

Screen, J. A., I. Simmonds, C. Deser, and R. Tomas, 2013: The Atmospheric Response to Three Decades of Observed Arctic Sea Ice Loss. *Journal of Climate*, **26 (4)**, 1230–1248, doi:10.1175/JCLI-D-12-00063.1, URL https://journals.ametsoc.org/view/journals/clim/26/4/jcli-d-12-00063.1.xml, publisher: American Meteorological Society Section: Journal of Climate.

Serreze, M. C., and R. G. Barry, 2011: Processes and impacts of Arctic amplification: A research synthesis. *Global and Planetary Change*, **77 (1)**, 85–96, doi:10.1016/j.gloplacha.2011.03.004, URL https://www.sciencedirect.com/science/article/pii/S0921818111000397.

Shields, C. A., and J. T. Kiehl, 2016: Atmospheric river landfall-latitude changes in future climate simulations. *Geophysical Research Letters*, **43 (16)**, 8775–8782, doi:10.1002/2016GL070470, URL https://onlinelibrary.wiley.com/doi/abs/10.1002/2016GL070470, _eprint: https://onlinelibrary.wiley.com/doi/pdf/10.1002/2016GL070470.

Shields, C. A., and Coauthors, 2018: Atmospheric River Tracking Method Intercomparison Project (ARTMIP): project goals and experimental design. *Geoscientific Model Development*, **11 (6)**, 2455–2474, doi:10.5194/gmd-11-2455-2018, URL

https://gmd.copernicus.org/articles/11/2455/2018/, publisher: Copernicus GmbH.

Simmonds, I., and I. Rudeva, 2012: The great Arctic cyclone of August 2012. *Geophysical Research Letters*, **39 (23)**, 2012GL054 259, doi:10.1029/2012GL054259, URL https://agupubs.onlinelibrary.wiley.com/doi/10.1029/2012GL054259.

Simpson, I. R., and Coauthors, 2020: An evaluation of the large-scale atmospheric circulation and its variability in cesm2 and other cmip models. *Journal of Geophysical Research: Atmospheres*, **125 (13)**, e2020JD032 835, doi:https://doi.org/10.1029/2020JD032835, URL https://agupubs.onlinelibrary.wiley.com/doi/abs/10.1029/2020JD032835, e2020JD032835 10.1029/2020JD032835, https://agupubs.onlinelibrary.wiley.com/doi/pdf/10.1029/2020JD032835.

Sousa, P. M., R. C. Blamey, C. J. C. Reason, A. M. Ramos, and R. M. Trigo, 2018: The 'Day Zero' Cape Town drought and the poleward migration of moisture corridors. *Environmental Research Letters*, **13 (12)**, 124 025, doi:10.1088/1748-9326/aaebc7, URL https://dx.doi.org/10.1088/1748-9326/aaebc7, publisher: IOP Publishing.

Sousa, P. M., A. M. Ramos, C. C. Raible, M. Messmer, R. Tomé, J. G. Pinto, and R. M. Trigo, 2020: North atlantic integrated water vapor transport—from 850 to 2100 ce: Impacts on western european rainfall. *Journal of Climate*, **33 (1)**, 263 – 279, doi:https://doi.org/10.1175/JCLI-D-19-0348.1, URL https://journals.ametsoc.org/view/journals/clim/33/1/jcli-d-19-0348.1.xml.

Stroeve, J., M. Serreze, S. Drobot, S. Gearheard, M. Holland, J. Maslanik, W. Meier, and T. Scambos, 2008: Arctic Sea Ice Extent Plummets in 2007.

Eos, Transactions American Geophysical Union, **89 (2)**, 13–14, doi:10.1029/2008EO020001, URL https://onlinelibrary.wiley.com/doi/abs/10.1029/2008EO020001, _eprint: https://onlinelibrary.wiley.com/doi/pdf/10.1029/2008EO020001.

Ullrich, P. A., C. M. Zarzycki, E. E. McClenny, M. C. Pinheiro, A. M. Stansfield, and K. A. Reed, 2021: TempestExtremes v2.1: a community framework for feature detection, tracking, and analysis in large datasets. *Geoscientific Model Development*, **14 (8)**, 5023–5048, doi:10.5194/gmd-14-5023-2021, URL https://gmd.copernicus.org/articles/14/5023/2021/, publisher: Copernicus GmbH.

Valkonen, E., J. Cassano, and E. Cassano, 2021: Arctic Cyclones and Their Interactions With the Declining Sea Ice: A Recent Climatology. *Journal of Geophysical Research: Atmospheres*, **126 (12)**, e2020JD034 366, doi:10.1029/2020JD034366, URL https://onlinelibrary.wiley.com/doi/abs/10.1029/2020JD034366, _eprint: https://onlinelibrary.wiley.com/doi/pdf/10.1029/2020JD034366.

Viale, M., R. Valenzuela, R. D. Garreaud, and F. M. Ralph, 2018: Impacts of Atmospheric Rivers on Precipitation in Southern South America. *Journal of Hydrometeorology*, **19 (10)**, 1671–1687, doi:10.1175/JHM-D-18-0006.1, URL https://journals.ametsoc.org/view/journals/hydr/19/10/jhm-d-18-0006_1.xml, publisher: American Meteorological Society Section: Journal of Hydrometeorology.

Waliser, D., and B. Guan, 2017: Extreme winds and precipitation during landfall of atmospheric rivers. *Nature Geoscience*, **10 (3)**, 179–183, doi:10.1038/ngeo2894, URL

https://www.nature.com/articles/ngeo2894, number: 3 Publisher: Nature Publishing Group.

Walsh, J. E., F. Fetterer, J. Scott stewart, and W. L. Chapman, 2017: A database for depicting Arctic sea ice variations back to 1850. *Geographical Review*, **107 (1)**, 89–107, doi:10.1111/j.1931-0846.2016.12195.x, URL https://doi.org/10.1111/j.1931-0846.2016.12195.x, publisher: Routledge _eprint: https://doi.org/10.1111/j.1931-0846.2016.12195.x.

Wang, Z., J. Walsh, S. Szymborski, and M. Peng, 2020: Rapid Arctic Sea Ice Loss on the Synoptic Time Scale and Related Atmospheric Circulation Anomalies. *Journal of Climate*, **33 (5)**, 1597–1617, doi:10.1175/JCLI-D-19-0528.1, URL https://journals.ametsoc.org/view/journals/clim/33/5/jcli-d-19-0528.1.xml, publisher: American Meteorological Society Section: Journal of Climate.

Wille, J. D., V. Favier, A. Dufour, I. V. Gorodetskaya, J. Turner, C. Agosta, and F. Codron, 2019: West Antarctic surface melt triggered by atmospheric rivers. *Nature Geoscience*, **12 (11)**, 911–916, doi:10.1038/s41561-019-0460-1, URL https://www.nature.com/articles/s41561-019-0460-1, number: 11 Publisher: Nature Publishing Group.

Wille, J. D., and Coauthors, 2021: Antarctic Atmospheric River Climatology and Precipitation Impacts. *Journal of Geophysical Research: Atmospheres*, **126 (8)**, e2020JD033 788, doi:10.1029/2020JD033788, URL https://onlinelibrary.wiley.com/doi/abs/10.1029/2020JD033788, _eprint: https://onlinelibrary.wiley.com/doi/pdf/10.1029/2020JD033788.

Woelders, L., J. T. M. Lenaerts, K. Hagemans, K. Akkerman, T. B. van Hoof, and W. Z. Hoek, 2018: Recent climate warming drives ecological change in a remote high-Arctic lake. *Scientific Reports*, **8 (1)**, 6858, doi:10.1038/s41598-018-25148-7, URL https://www.nature.com/articles/s41598-018-25148-7, number: 1 Publisher: Nature Publishing Group.

Yang, W., and G. Magnusdottir, 2017: Springtime extreme moisture transport into the arctic and its impact on sea ice concentration. *Journal of Geophysical Research: Atmospheres*, **122 (10)**, 5316–5329, doi:https://doi.org/10.1002/2016JD026324, URL https://agupubs.onlinelibrary.wiley.com/doi/abs/10.1002/2016JD026324, https://agupubs.onlinelibrary.wiley.com/doi/pdf/10.1002/2016JD026324.

Zhang, P., G. Chen, W. Ma, Y. Ming, and Z. Wu, 2021: Robust Atmospheric River Response to Global Warming in Idealized and Comprehensive Climate Models. *Journal of Climate*, **34 (18)**, 7717–7734, doi:10.1175/JCLI-D-20-1005.1, URL https://journals.ametsoc.org/view/journals/clim/34/18/JCLI-D-20-1005.1.xml, publisher: American Meteorological Society Section: Journal of Climate.

Zhang, P., G. Chen, M. Ting, L. Ruby Leung, B. Guan, and L. Li, 2023: More frequent atmospheric rivers slow the seasonal recovery of Arctic sea ice. *Nature Climate Change*, **13 (3)**, 266–273, doi:10.1038/s41558-023-01599-3, URL https://doi.org/10.1038/s41558-023-01599-3.

Zhao, M., 2020: Simulations of atmospheric rivers, their variability, and response to global warming using gfdl's new high-resolution general circulation model. *Journal*

of Climate, **33 (23)**, 10 287 – 10 303, doi:https://doi.org/10.1175/JCLI-D-20-0241.1, URL https://journals.ametsoc.org/view/journals/clim/33/23/jcliD200241.xml.

Zhu, Y., and R. E. Newell, 1998: A proposed algorithm for moisture fluxes from atmospheric rivers. *Monthly Weather Review*, **126 (3)**, 725 – 735, doi:https://doi.org/10.1175/1520-0493(1998)126⟨0725:APAFMF⟩2.0.CO;2, URL https://journals.ametsoc.org/view/journals/mwre/126/3/1520-0493_1998_126_0725_apafmf_2.0.co_2.xml.